diseases

MDPI

Article

Premature Neuroimmune and Redox-Inflammatory Breakdown at the Prodromal Stage in Male and Female Triple-Transgenic Alzheimer's Disease Mice

Lydia Giménez-Llort [1,2,*,†], Carmen Vida [3], Judith Félix [3], Silvia Quer-Palomas [1,2], Rashed Manassra [3] and Monica De la Fuente [3,4,†]

[1] Institut de Neurociències, Universitat Autònoma de Barcelona, 08193 Barcelona, Spain; silvia.quer@autonoma.cat
[2] Department of Psychiatry and Forensic Medicine, School of Medicine, Universitat Autònoma de Barcelona, 08193 Barcelona, Spain
[3] Department of Genetics, Physiology and Microbiology, Faculty of Biological Sciences, Complutense University of Madrid, 28040 Madrid, Spain; carmenvida@ucm.es (C.V.); jufelix@ucm.es (J.F.); rashed.manassra@ucm.es (R.M.); mondelaf@ucm.es (M.D.l.F.)
[4] Institute of Investigation Hospital 12 Octubre (imas12), 28041 Madrid, Spain
* Correspondence: lidia.gimenez@uab.cat; Tel.: +34-93-5812378
† These authors contributed equally to this work.

Abstract

Background/Objectives: Homeostatic (nervous, immune and endocrine) systems and their communications network are crucial for health and aging rate. We previously reported behavioral and peritoneal leukocyte function alterations and oxidative-inflammatory stress in young female triple-transgenic (3xTg) mice for Alzheimer's disease (AD). Here, the deterioration of the homeostatic systems and their interplay was investigated, in an integrated way, at prodromal stages and in both sexes of 3xTg-AD mice. Methods: An integrative analysis of the behavioral profile, peripheral immune splenic and thymic leukocyte functions, splenic oxidative-inflammatory state, and plasmatic corticosterone in both sexes of 3xTg-AD mice at 4 months of age was compared to that of age- and sex-matched NTg counterparts. Results: The prodromal stage of 3xTg-AD, characterized by anxiety-like behaviors and disrupted exploration, was aligned with reduced chemotaxis, natural killer activity, and lymphoproliferation—especially in the spleen. In addition, 3xTg-AD mice exhibited lower anti-inflammatory (IL-10) and higher pro-inflammatory (IL-2, IL-1β, and TNF-α) cytokine concentrations and oxidative stress (higher oxidants and lower antioxidants). Several of these alterations displayed sex-dependent differences (worse in males). However, no differences in corticosterone were found. Conclusions: These findings suggest that neuroimmune and redox-inflammatory dysfunctions, indicative of premature aging, emerge at the prodromal stage of AD, preceding corticosterone changes, unveiling a time lag in the neuroimmunoendocrine alterations in these animals. They may act as early indicators of premature aging in AD pathology and provide potential targets for sex-specific prodromal intervention.

Keywords: Alzheimer's disease; 3xTg-AD mice; prodromal stage; behavior; immune functions; oxidative-inflammatory stress; corticosterone; neuroimmunoendocrine communications; spleen; thymus; males and females; premature aging

Academic Editor: Christian Barbato

Received: 26 December 2025
Revised: 30 January 2026
Accepted: 3 February 2026
Published: 9 February 2026

1. Introduction

More than 30 million individuals suffer from Alzheimer's disease (AD), the most prevalent chronic neurodegenerative disorder, which is primarily distinguished by extracellular amyloid beta plaques and intracellular neurofibrillary tangles, resulting in impaired synaptic function, neuronal loss, cognitive decline, and neuropsychiatric symptoms [1]. In the coming years, the burden of AD and its economic impact will dramatically increase with the aging of the population [2]. Despite decades of research, there are no effective therapies to address the many cellular and molecular alterations of this neurological disorder [3,4]. For this reason, an increasing number of studies have focused on the disclosure of AD pathology before the onset of dementia, trying to find prodromal peripheral markers that allow for intervention before the disease is in an advanced stage [5–7].

In this context, we must consider the essential role of homeostatic systems, such as the nervous, immune, and endocrine systems, and their communication to ensure adaptive mechanisms and, therefore, health maintenance. This neuroimmunoendocrine network is fundamental for successful aging and longevity. Thus, its deterioration, which is underpinned by an oxidative-inflammatory stress state, generated in part by the immune system, supposes a premature or accelerated aging as well as an increased risk of morbidity and mortality [8].

Currently, there is emerging research on the relevance of immunity in Alzheimer's disease, contributing to neuroinflammation and oxidative stress, both within the central nervous system and in the periphery. Thus, the role of the peripheral immune system in this neurodegenerative disease seems evident. In fact, it has been proposed that the involvement of the bidirectional communication between peripheral immune cells and the central nervous system (CNS) accelerates neuroinflammation and cognitive decline [9–13]. Moreover, we have found that several functions of peripheral blood immune cells can serve as markers of AD progression [14].

The late clinical onset of AD in most affected people is a limitation for clinical research when deciphering the cellular and molecular changes at the preclinical (asymptomatic and prodromal) stages of the disease. For this reason, animal models, especially genetic mouse models of AD, are very useful for studying its pathogenesis. Although there are many mouse models of AD [15,16], the triple-transgenic mouse for Alzheimer's disease (3xTg-AD), harboring PS1M146V, APPSwe, and tauP301L transgenes, represents an interesting model [17]. It mimics many critical hallmarks of AD neuropathology, such as both amyloid-beta and tau neuropathology in an age-dependent manner and in disease-relevant brain regions, reproducing a similar temporally and anatomically specific profile observed in humans. This model presents synaptic and cholinergic deficits, the characteristic reactive gliosis inflammatory profile, as well as cognitive impairment [18–25]. In addition, since our first reports [26], we have consistently proposed the 3xTg-AD mouse as a model of special interest to study neuropsychiatric-like symptoms of dementia since it exhibits several behavioral alterations already before the early signs of intraneuronal beta-amyloid that worsen in an age-dependent manner along with changes at the neuroanatomical level [27].

The crosstalk between behavior (an indicator of nervous function) and the peripheral immune system plays a crucial role, particularly during the prodromal stages of disease [28]. In a previous longitudinal study carried out only in female 3xTg-AD mice, we analyzed several functions of peritoneal immune cells [29,30], but the functional state of their spleen and thymus leukocytes was assessed at the end point, older age [31,32]. Moreover, in this model, splenomegaly, histopathological changes and splenic dysfunction have been associated with advanced stages of disease [33–35]. However, the state and interplay of the components of the neuroimmunoendocrine system in these 3xTg-AD mice have not been studied in an integrated way at an early stage of the disease.

As mentioned before, oxidative stress has been considered a crucial central factor in the pathogenesis of AD, as a bridge that connects the different mechanisms of this disease [36], and it is an early event in AD progression. Thus, compared with the corresponding NTg mice, peritoneal immune cells of 2-month-old 3xTg-AD female mice showed oxidative stress and higher lipid peroxidation [29,30]. Moreover, a higher presence of oxidants has been observed in the brain and serum [37,38] of these animals at 2–3 months of age. However, in several parameters, these differences disappear after 6 months of age. In addition, inflammatory stress (higher presence of pro-inflammatory than the anti-inflammatory compounds), a process associated with oxidative stress [39], is a common feature in both the brain and the peripheral immune system, contributing to pathogenesis and progression of AD [40]. In the 3xTg-AD mice, higher brain pro-inflammatory mediator expression has been observed at 6 and 12 months of age following parasitic infection [41]. In peritoneal immune cells of 3xTg-AD female mice, higher ratios of pro-inflammatory/anti-inflammatory concentrations in 3xTg-AD than in NTg mice at 2 and 4 months have been observed [30]. Nevertheless, the oxidative and inflammatory stress in immune organs at a prodromal stage of the disease is unknown. Finally, a relevant endocrine component in neuroimmune communication, the corticosterone hormone, which is also related to an inflammatory state, has been studied in 3xTg-AD mice at old ages [31] or in a social isolation stress response [42], but its plasma concentrations in these mice at 4 months of age have not been analyzed.

The typical age-related deterioration of the homeostatic systems and their communication, which is associated with an oxidative-inflammatory stress, is involved in the rate of aging and longevity [8] and can appear at a young age and in adults. Thus, in several murine models of premature aging, which is related to a shorter lifespan of these animals than that of their age-matched controls, premature alterations in behavioral responses, immunosenescence, and oxi-inflammaging have been observed [39,43]. However, in these young or adult animals that prematurely age, intervention with healthy lifestyle strategies allows their successful aging and greater longevity [39]. In this context, it is interesting to know the peripheral markers of immune, redox, and inflammatory states at early ages in 3xTg-AD in order to have a better basis to test strategies to prevent or delay the symptoms of this disease.

Regarding sex-dependent differences observed in AD [44,45], these are relevant to neuroimmunoendocrine communication and the longevity of animals, including humans and mice [34,46]. In 3xTg-AD mice, sex differences have been observed in cerebral pathology and behavioral responses, as well as in several aspects of immunity and oxidative-inflammatory state [47–52]. Finally, considering the early BPSD-like profile of this animal model [26–28], including endocrine outcomes referred to the HPA axis is relevant for our integrative approach to study the homeostasis systems. Female 3xTg-AD mice exhibit significantly higher basal and stress-induced corticosterone levels compared to males [51], but we have also demonstrated that at advanced stages, a worse endocrine modulation in males results in a lack of sex differences in this respect [31].

For all the above-mentioned reasons, the present work aimed to perform an integrative study on the emergence of dysfunctions in the different components of the psychoneuroimmunoendocrine network in male and female 3xTg-AD mice at the prodromal stage (4 months of age) of the disease. Thus, their prodromal state was verified by several behavioral parameters, the endocrine system by analyzing plasma corticosterone concentrations and weight of adrenal glands, and the immune system by studying several leukocyte functions (chemotaxis, natural killer activity, lymphoproliferation, and cytokine release). Moreover, since the base neuroimmunoendocrine alterations are an oxidative-inflammatory stress, several markers of this stress were also measured.

2. Materials and Methods

2.1. Animals

Four-month-old male and female 3xTg-AD mice from the Spanish colony of homozygous 3xTg-AD mice, established in the Medical Psychology Unit, Universitat Autònoma de Barcelona, were used in the present study. The 3xTg-AD mouse strain harboring the familial AD mutations PS1M146V, APPswe, and tauP301L transgenes was genetically engineered at the University of California, Irvine, as previously described [17,18]. The non-transgenic (NTg) mouse colony had the same genetic hybrid background (129 × C57BL6) as 3xTg-AD mice. Genotypes were confirmed by polymerase chain reaction (PCR) analysis of DNA obtained from tail biopsies. Three to five littermates of the same genotype and sex were maintained in Macrolon cages (Techniplast, Buguggiate, Italy, 35 cm × 35 cm × 25 cm) under standard laboratory conditions of food and water ad libitum, temperature (22 ± 2 °C) and humidity (50–60%), on a 12/12 h light/dark cycle (lights on at 08:00). Estrous cycle of the female mice was not determined to avoid stressing the animals by the vaginal smear analyses. However, it is known that most female mice housed in groups in the same room spontaneously synchronize their estrous cycles [53]. This reduced the possibility of a hormone bias in the comparison of the different experimental groups.

2.2. Experimental Design

Thirty-eight 3xTg-AD mice and sex- and age-matched NTg mice were assessed for behavior responses in the corner test for neophobia (CT), open-field test (OF), and T-maze (TM) [26], which were evaluated by direct observation and VideoTrack analysis system (ViewPoint Behavior Technology, Lyon, France). Experiments were conducted under dim white-light conditions (16–20 lux) from 10:00 a.m. to 1:00 p.m. Two days after the behavioral assessment, the animals were sacrificed by decapitation to obtain blood immediately, and the target samples (thymus, spleen, and adrenal glands) were removed and weighed. In the case of the spleen and thymus, they were divided into two parts. One was rapidly frozen and stored at −80 °C until the redox state assays were performed, and the other was used to obtain the leukocytes, as described below.

All the experiments were conducted in accordance with the Spanish legislation on "Protection of Animals Used for Experimental and Other Scientific Purposes" and the EU Directive (2010/63/EU) on this subject, and the Ethical Commission of the Universitat Autònoma de Barcelona (Protocol Number CEEAH/00759 3588/DMAH 9452).

2.3. Prodromal Behavioral Profile

The prodromal behavioral state of animals was assessed by means of a battery of three tests:

Corner test for neophobia (CT): The fear of a new home-cage was assessed by introducing the animal into the center of the standard cage (Macrolon, 35 cm × 35 cm × 25 cm) and counting the number of visited corners and rearings during a period of 30 s. Latency to the first rearing was also recorded [26].

Open-field test (OF): Mice were placed in the center of the apparatus (homemade, wooden, white, 50 cm × 50 cm × 25 cm high) and observed for 5 min. Horizontal (crossings of 10 cm × 10 cm squares) and vertical (number of rearings) locomotor activities were recorded for each minute of the test. We also recorded the ethogram, the latency of the sequence of the following behavioral events: initial freezing (latency of initial movement), thigmotaxis or discrimination of unprotected/protected areas in the test (latency of leaving the central 10 cm × 10 cm square and that of entering in the peripheral ring 5 cm to the walls), and self-grooming behavior (latency, number, and duration of grooming). Emotionality (defecation and the presence/absence of urine) was also measured [51].

T-maze (TM): The spontaneous exploratory behavior and alternation of mice were tested in a T-shaped maze with "horizontal" arms 25 cm in length. Animals were placed inside the "vertical" arm of the maze (35 cm in length) with their head facing the end wall. The coping with stress strategies performance was evaluated by determining the time elapsed until the animal crossed (four-paw criteria) the intersection of the three arms [43]. The test was completed once the animal had finished exploring the two "horizontal arms". The exploratory efficiency was measured by means of different variables: the total time invested to complete the maze exploration, the number of errors (revisiting an arm) made, and the ratio between arms (time needed to complete the test divided by the latency to reach the intersection). Emotionality (defecation and the presence/absence of urine) was also recorded [43].

2.4. Organometrics

The size (weight in mg) and relative size (% vs. body weight) of peripheral immunoendocrine organs, including the thymus, spleen, and adrenal glands, were recorded during the harvesting, before the analysis of peripheral immune functions and corticosterone assay [51].

2.5. Immune Functions

2.5.1. Collection of Lymphocyte Suspensions

Spleen and thymus were removed aseptically, freed of fat, minced with scissors, and gently pressed through a mesh screen (Sigma-Aldrich, St. Louis, MO, USA). The collection of lymphocytes was assessed according to the method previously described [43]. Spleen suspensions, due to their high concentration of erythrocytes, were centrifuged in a gradient of Ficoll-Hypaque (Sigma-Aldrich) with a density of 1.070 g/mL. Cells were recollected from the interface and resuspended in complete medium (containing RPMI 1640 enriched with L-glutamine and phenol red and supplemented with 10% heat-inactivated (56 °C, 30 min) fetal calf serum (Hyclone, GE Healthcare, Logan, UT, USA) and gentamicin (100 mg/mL, Sigma-Aldrich)). Lymphocytes were washed, and their number was determined and adjusted to 10^6 cells/mL. Cellular viability, routinely measured before and after each experiment by the Trypan-Blue exclusion test, was higher than 98% in all experiments. All incubations were performed at 37 °C in a humidified atmosphere of 5% CO_2.

2.5.2. Chemotaxis Assay

The induced mobility or chemotaxis of leukocytes was evaluated according to the method previously described [43]. Chambers with two compartments, separated by a 3 µm pore diameter filter (Millipore, County Cork, Ireland), were used. Aliquots of 300 µL of splenic or thymic lymphocyte suspensions adjusted to 10^6 cells/mL in Hank's medium were deposited in the upper compartment, and 400 µL of the chemoattractant agent formyl-methionyl-leucine-phenylalanine (f-met-leu-phe, Sigma-Aldrich) at a concentration of 10–8 M was deposited in the lower compartment. The chambers were incubated for 3 h, the filters were fixed and stained, and the number of lymphocytes on one-third of the lower face of the filter (corresponding to five scans of 5 mm) was counted using an optical microscope (×100 magnification) and recorded as Chemotaxis Index (C.I.).

2.5.3. Natural Killer (NK) Cytotoxicity Assay

The NK cell cytotoxicity, which is the main antitumoral protection of the organism, was measured by an enzymatic colorimetric assay (Cytotox 96^{TM} Promega, Boehringer Ingelheim, Germany) based on the determination of lactate dehydrogenase (LDH) released by the cytolysis of target cells (YAC-1 cells from a murine lymphoma), using tetrazolium

salts (ID) [43]. Briefly, target cells were seeded in 96-well U-bottom culture plates (Nunclon, Roskilde, Denmark) at 10^4 cells/well in 1640 RPMI medium without phenol red (Gibco, Waltham, MA, USA). Effector cells (splenic or thymic lymphocyte suspensions adjusted to 10^6 cells/mL) were added at 105 cells/well, obtaining an effector/target rate of 10/1. The plates were centrifuged at 250× *g* for 5 min to facilitate cell-to-cell contacts and were incubated for 4 h at 37 °C. After incubation, LDH activity was measured in 50 µL/well by adding the enzyme substrate, with absorbance recorded at 490 nm. The results were expressed as the percentage of tumor cells killed (% lysis).

2.5.4. Lymphoproliferation Assay

The proliferation capacity of lymphocytes was evaluated by a standard method previously described [43]. The assay was assessed in basal and stimulated conditions using the mitogens concanavalin A (Con-A) and lipopolysaccharide (LPS). Aliquots of 200 µL of splenic or thymic leukocyte (mainly lymphocytes) suspensions adjusted to 10^6 cells/mL in complete medium were dispensed into 96-well plates (Nunclon, Denmark). A 20 µL volume of complete medium (basal lymphoproliferation), Con-A or LPS (1 µg/mL, Sigma-Aldrich) was added to each well. After 48 h of incubation at 37 °C in a sterile and humidified atmosphere of 5% CO_2, 0.5 µCi 3H-thymidine (Hartmann Analytic, Blaubeuren, Germany) was added to each well. Previously, 100 µL of culture supernatant from each well was collected and stored at −80 °C until used for harvesting in a semiautomatic harvester (Skatron Instruments, Lillestrøm, Norway). Thymidine uptake was then measured using a beta counter (LKB, Uppsala, Sweden) for 1 min. The results were calculated as 3H-thymidine uptake (counts per minute, c.p.m.) for basal and stimulated (with mitogens) conditions and were also expressed as lymphoproliferation capacity (%), giving 100% to the c.p.m in basal conditions.

2.5.5. Cytokine Concentrations in Cultures of Spleen Leukocytes

The release of interleukin-2 (IL-2), interleukin-10 (IL-10), interleukin-1beta (IL-1β), and tumor necrosis factor alpha (TNF-α) was measured in culture supernatants of splenic lymphocytes after 48 h of incubation in the presence of Con-A (1 µg/mL) or LPS (1 µg/mL) as described above. Levels of IL-2, IL-10, IL-1β, and TNF-α were measured simultaneously by multiplex luminometry (MILLIPLEX® MAP Mouse Cytokine/Chemokine kit, Immunoassay, Millipore, Billerica, MA, USA). Each assay was run in duplicate. The minimum detectable concentration of IL-2, IL-10, IL-1β, and TNF-α was 3.2 pg/mL. The results were expressed in picograms per milliliter (pg/mL).

2.6. Redox-Inflammatory State

2.6.1. Glutathione Peroxidase (GPx) Activity

The GPx activity was spectrophotometrically evaluated in homogenates of the spleen according to the method described by Lawrence and Burk [54], with some modifications. Briefly, tissue samples of spleen were homogenized (50 mg/mL) with tampon phosphate (50 mM, pH 7.4), being maintained on ice during the entire process. Thereafter, homogenates were centrifuged at 3200× *g* for 20 min at 4 °C. Aliquots of the supernatants were measured in the spectrophotometer using cumene hydroperoxide (cumene-OOH, Sigma-Aldrich) as substrate, which carried out the oxidation of glutathione, which is regenerated by the addition of β-nicotinamide adenine dinucleotide phosphate, in its reduced form (β-NADPH, Sigma-Aldrich), in the presence of glutathione reductase (GR, 10 U/mL, Sigma-Aldrich). The reaction was monitored spectrophotometrically by measuring the decrease in absorbance at 340 nm every 40 s over 5 min. The results were expressed as international milliunits of enzymatic activity per mg of tissue (mU GPx/mg tissue).

2.6.2. Glutathione Reductase (GR) Activity

The GR activity was spectrophotometrically assessed in homogenates of the spleen according to the method described by Massey and Williams [55], with some modifications. Briefly, tissue samples of the spleen were homogenized in a tampon phosphate solution (50 mM, pH 7.4) containing EDTA (6.3 mM). Homogenates were centrifuged at 3200× *g* for 20 min at 4 °C. Aliquots of the supernatants were measured in the spectrophotometer using the β-NADPH (6 mM) and oxidized glutathione (GSSG, 80 mM, Sigma-Aldrich) reagents. The reaction was monitored spectrophotometrically by measuring the decrease in absorbance at 340 nm every 40 s over a 4-min period. The results were expressed as international milliunits of enzymatic activity per mg of tissue (mU GR/mg tissue).

2.6.3. Total Glutathione (GSH) Content

Total glutathione (GSH), the main non-enzymatic reducing agent of the organism, was assayed by the previously described enzymatic recycling method by monitoring the change in absorbance at 412 nm, with some modifications in organs [43]. Briefly, samples of spleen were homogenized (50 mg/mL) with 5% trichloroacetic acid (TCA, Panreac, Barcelona, Spain) and 0.01 N HCl (Panreac, Barcelona, Spain), being maintained on ice throughout the process. Homogenates were centrifuged at 3200× *g* for 5 min at 4 °C. Aliquots of the supernatants were measured in the spectrophotometer using the following reaction mixture: 5,5′-dithiobis-(2-nitrobenzoic acid) (DTNB, 6 mM, Sigma-Aldrich), β-nicotinamide adenine dinucleotide phosphate, reduced form (β-NADPH, 0.3 mM, Sigma-Aldrich), and glutathione reductase (GR, 10 U/mL, Sigma-Aldrich). The reaction was monitored for 240 s, and the results were expressed as nanomoles of GSH per mg of tissue (nmol GSH/mg tissue).

2.6.4. Xanthine Oxidase (XO) Activity

The XO activity was assayed in homogenates of spleen by fluorescence using a commercial kit (Amplex Red Xanthine/Xanthine Oxidase Assay Kit, Molecular Probes, Paisley, UK) [43]. In the assay, XO catalyzes the oxidation of purine bases (xanthine) to uric acid and superoxide. The superoxide spontaneously degrades in the reaction mixture to H_2O_2, which, in the presence of horseradish peroxidase (HRP), reacts stoichiometrically with Amplex Red reagent to generate the red-fluorescent oxidation product, resorufin. Tissue samples of the spleen were homogenized in phosphate buffer (50 mM, pH 7.4) containing EDTA (1 mM) and normalized according to total protein. The homogenates were centrifuged at 5000× *g* for 30 min at 4 °C. Aliquots of the supernatants (50 µL) were incubated with 50 µL working solution of Amplex Red reagent (100 µM) containing HRP (0.4 U/mL) and xanthine (200 µM). After 30 min of incubation at 37 °C, fluorescence measurement was performed using a microplate reader (Fluostar Optima, BMG Labtech, Ortenberg, Germany; Biomedal, Sevilla Spain) with excitation at 530 nm and emission detection at 595 nm. The XO supplied in the kit was used as the standard, and XO activity was measured by comparing the fluorescence of the samples with that of the standards. The protein content of the same samples was evaluated using the bicinchoninic acid protein assay kit protocol (Sigma-Aldrich, St. Louis, MO, USA), with serum albumin (BSA, Sigma-Aldrich, St. Louis, MO, USA) as the standard. The results were expressed as international milliunits (mU) of enzymatic activity per milligram of protein (mU XO/mg protein).

2.7. Plasma Corticosterone

Samples of about 1 mL of whole trunk blood were collected at the time of sacrifice into heparinized tubes and centrifuged immediately at 10,000× *g* for 2 min. The plasma obtained was stored at −20 °C. Corticosterone content (ng/mL) was analyzed using a

commercial kit (Corticosterone EIA Immunodiagnostic Systems Ltd., Boldon, UK) and ELISA EMSReader MFV.2.9-0.6 [51,56].

2.8. Statistical Analysis

Statistical analysis was performed in SPSS IBM 29.0 (SPSS, Chicago, IL, USA) and GraphPad Prism 10.1.1 (LLC, San Diego, CA, USA). The results are presented as the mean ± standard error (SEM). Normality of the samples and homogeneity of the variances were checked by the Kolmogorov–Smirnov test and Levene's test, respectively. All tests were two-tailed. Differences were studied through two-way ANOVA. The factors were genotype and sex. The Tukey test was used for post hoc comparisons when variances were homogeneous, whereas its counterpart, the Games–Howell analysis, was used in the case of unequal variances. In all cases, $p < 0.05$ was taken as statistically significant.

3. Results

3.1. Prodromal Behavioral State of 4-Month-Old Male and Female 3xTg-AD Mice

The study first verified the prodromal behavioral state of the 3xTg-AD mice as compared to sex-matched counterparts. Thus, the behavioral profile exhibited by the animals in the three behavioral tests was analyzed in terms of genotype, sex, and interaction effects, as summarized in Table 1. Thereafter, among the main variables showing statistically significant effects (as illustrated in Figure 1), the most sensitive variables to these factors were identified.

The first BPSD-like symptoms were already apparent in the 3xTg-AD mice. The sensitivity of the corner test for neophobia to define the prodromal stage of 3xTg-AD mice was shown as a higher anxiety-like response than observed in the NTg mice, which could be measured not only by the latency (Table 1, G **, $p < 0.01$) but also by a lower number of rearings (Table 1, G ***, $p < 0.001$). As illustrated in Figure 1a, this neophobia reached the highest levels in male 3xTg-AD mice as compared to all the other groups (** $p < 0.01$ vs. NTg counterparts; ++ $p < 0.01$ vs. female counterparts).

When the animals were confronted with the open-field test, 3xTg-AD mice showed higher latencies in most of the behavioral events (Table 1, G *, $p < 0.05$). The incidence of bizarre behavior in the male and female 3xTg-AD mice was higher than in NTg mice (males, *** $p < 0.001$ and females, * $p < 0.5$, respectively). Statistically significant differences in the time course of the vertical component (rearings) were recorded, mostly in females in minutes 2 and 3 (* $p < 0.05$). Exhibition of emotionality was lower in 3xTg-AD mice (Table 1, G *, $p < 0.05$) and male sex (S **, $p < 0.01$). Here and in the T-maze, NTg females showed a statistically significantly higher number of defecations as compared to all the other groups ($p < 0.05$).

In the T-maze, genotype differences were observed in the latency to reach the intersection (Table 1 and Figure 1h, G *, $p < 0.05$). Post hoc tests indicated that 3xTg-AD female mice exhibited statistically significantly higher values compared to all other groups. The genotype effect could also be observed when the ratio between the time spent in the vertical and horizontal arms was considered (Table 1, * $p < 0.05$), while the total time invested in completing the maze exploration (Table 1) did not differ between groups. A genotype × sex interaction effect could be found in the number of errors (Figure 1i and Table 1, G × S *, $p < 0.05$). The emotionality showed sex differences, with females producing more defecation boli and exhibiting a higher incidence of urination. This sex effect was primarily due to female NTg mice, which exhibited a higher number of these behaviors compared to all other groups (Figure 1j and Table 1, $p < 0.05$).

Table 1. Behavioral profile in 4-month-old female and male 3xTg-AD and NTg mice.

Behavioral Tests	NTg		3xTg-AD		Factor Analysis G, Genotype S, Sex
	Females (n = 11)	Males (n = 9)	Females (n = 8)	Males (n = 10)	
Corner Test					
Ethogram (Sequence of behavioral events)					
Vertical activity (latency, s)	5.72 ± 0.96	7.22 ± 2.73	9.5 ± 1.2	20.7 ± 2.58 **++	G **, S **, G × S *
Locomotor activity					
Horizontal activity (corners, n)	13.73 ± 0.98	11.89 ± 1.29	11.25 ± 2.66	8.20 ± 1.42	n.s., n.s., n.s.
Vertical activity (rearings, n)	6.36 ± 0.47	7.22 ± 1.26	4.38 ± 1.02	2.30 ± 0.63	G ***, n.s., n.s.
Open Field Test					
Ethogram (Sequence of behavioral events)					
Initial movement (latency, s)	1.36 ± 0.28	0.33 ± 0.17	2.50 ± 0.53 *	1.10 ± 0.38	G *, n.s., n.s.
Incidence of bizarre behavior (%)	55.9 ± 12	9.69 ± 11 ++	76.3 ± 11 *	100 ± 0 *** ++	G ***, S **, G × S **
Exit from the center (latency, s)	6.27 ± 0.63	5.66 ± 1.3	14.37 ± 3.38 **	8.9 ± 1.96 **	G **, n.s., n.s.
Entrance to periphery (latency, s)	15.36 ± 2.04	49.4 ± 16.5	48.8 ± 27.6	24.2 ± 5.05	n.s., n.s., G × S **
Vertical activity (latency, s)	32.18 ± 2.88	46.2 ± 10.2	72.1 ± 27.1 *	74.6 ± 21.0	G *, n.s., n.s.
Self-grooming (latency, s)	142.73 ± 18.16	188.33 ± 20.8	231.88 ± 22.48 *	201.3 ± 20.08	G *, n.s., n.s.
Locomotor activity					
Vertical activity per minute (rearings, n)	r1: 3.82 ± 0.58 r2: 3.36 ± 0.51 r3: 2.73 ± 0.49 r4: 2.09 ± 0.69 r5: 1.64 ± 0.7	r1: 2.33 ± 0.59 r2: 2.33 ± 0.68 r3: 3 ± 0.71 r4: 3.22 ± 0.56 r5: 3 ± 0.61	r1: 1.75 ± 0.82 r2: 0.88 ± 0.3 * r3: 1.13 ± 0.4 * r4: 1.13 ± 0.4 + r5: 1.5 ± 0.38	r1: 2.1 ± 0.63 r2: 1.6 ± 0.59 r3: 2.1 ± 0.5 r4: 2.7 ± 0.71 r5: 2.5 ± 0.85	G *, n.s., n.s./ G *(r2, r3) S *(r4) n.s.
Total vertical activity (rearings, n)	13.55 ± 1.04	13.89 ± 2.57	6.37 ± 1.43 *	11 ± 2.98	n.s., n.s., n.s.
Self-grooming behavior					
Self-grooming episodes (n)	1.36 ± 0.20	1.33 ± 0.37	0.75 ± 0.25	1.20 ± 0.25	n.s., n.s., n.s.
Total self-grooming duration (s)	4.55 ± 0.73	4.00 ± 0.85	2.50 ± 0.76	4.40 ± 0.79	n.s., n.s., n.s.
Emotionality					
Defecation boli (n)	4.1 ± 0.55	1.56 ± 0.43 ++	2 ± 0.57 *	1.4 ± 0.47	G *, S **, n.s.
Urination (incidence)	0.27 ± 0.14	0 ± 0	0.25 ± 0.16	0.30 ± 0.15	n.s., n.s., n.s.
T-maze					
Ethogram (Sequence of behavioral events)					
Reaching intersection (latency, s)	11 ± 1.96	11.8 ± 2	59.6 ± 26.8 **	21.5 ±11.4	G *, n.s., n.s.
Exploratory efficiency (time, s)	44.55 ± 14.3	56.0 ± 12.6	88.0 ± 27.3	36.3 ± 12.0	n.s., n.s., n.s.
Ratio time in the arms (s)	4.31 ± 0.77	4.90 ± 0.72	2.86 ± 0.63 *	2.69 ± 0.37 *	G **, n.s., n.s.
Errors (n)	0.36 ± 0.2	0.78 ± 0.28	1 ± 0.5 *** ++	0.2 ± 0.13 *** +++	G ***, n.s., G × S *
Emotionality					
Defecation boli (n)	1.27 ± 0.43	0.33 ± 0.17 +++	1.37 ± 0.53	0.3 ± 0.21 +++	n.s., S **, n.s.
Urination (incidence)	0.55 ± 0.21	0 ± 0	0.12 ± 0.12	0.10 ± 0.10	n.s., n.s., n.s.

Results are the mean ± SEM of 8–11 animals. Statistics: Factor analysis: * $p < 0.05$, ** $p < 0.01$, and *** $p < 0.001$ vs. NTg (G, genotype effects), or female mice (S, sex effects), or in the comparison to genotype × sex effects (G × S); n.s., non-statistically significant differences. Post hoc analysis: * $p < 0.05$, ** $p < 0.01$, *** $p < 0.001$ vs. NTg group with the same sex; + $p < 0.05$, ++ $p < 0.01$, +++ $p < 0.001$ vs. female group with the same genotype. NTg: non-transgenic mice; 3xTg-AD: triple transgenic mice for Alzheimer's disease.

Therefore, the factorial analysis (as detailed in Table 1) pointed out the strong predominance of genotype factor, as it was observed in most of the variables studied, but also revealed their different magnitudes of sensitivity to these factors (Table 1, from G *, $p < 0.05$ to G ***, $p < 0.001$). Sex differences (S **, $p < 0.01$) were found in emotionality related variables such us the latency of vertical activity in the corner test (Figure 1a and Table 1, S **, $p < 0.01$), the incidence of bizarre behaviors in the open-field test (Figure 1b and Table 1, S **, $p < 0.01$) and the defecatory behavior in the open-field test and the T-maze (Figures 1g and 1j, respectively; Table 1, S ** $p < 0.01$). With regard to variables sensitive to one or both factors or their interaction, the time course of the vertical activity (Figure 1e)

was sensitive to genotype (rearing on minute 2 and 3, both G *, $p < 0.05$) and sex (rearings on minute 4, S *, $p < 0.05$). Some variables also showed genotype per sex interaction effects (G × S *, $p < 0.05$ and G × S **, $p < 0.01$).

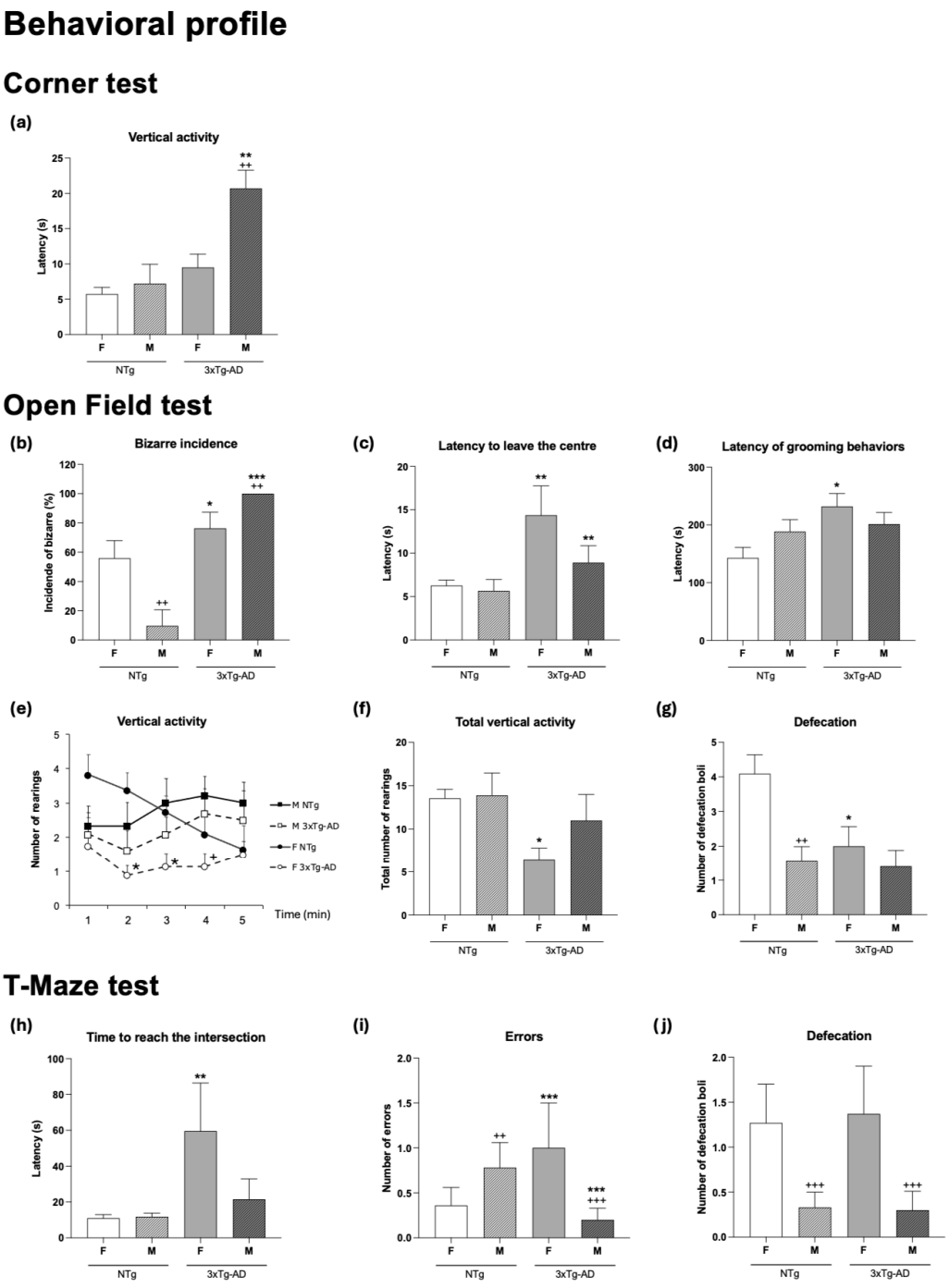

Figure 1. Prodromal behavioral profile of 4-month-old female (F) and male (M) non-transgenic (NTg) and triple transgenic for Alzheimer's disease (3xTg-AD) mice. Corner test: (**a**) Latency of vertical activity (rearings); Open-field test: (**b**) bizarre incidence (%); (**c**) latency to leave the center; (**d**) latency of grooming; (**e**) vertical activity (number of rearings in each minute of the test); (**f**) total vertical activity (total number of rearings), (**g**) number of defecation boli. T-maze: (**h**) latency to reach the intersection; (**i**) number of errors; (**j**) number of defecation boli. Each column represents the mean ± SEM of 8–11 values corresponding to the same number of subjects (NTg mice: 11 females, 9 males; 3xTg-AD mice: 8 females, 10 males). Each value is the mean of duplicate assays. Statistics: * $p < 0.05$, ** $p < 0.01$, *** $p < 0.001$ vs. NTg group with the same sex; + $p < 0.05$, ++ $p < 0.01$, +++ $p < 0.001$ vs. female group with the same genotype.

In summary, at this prodromal stage, the behavioral variables most sensitive to genotype, sex and interaction effects were (1) the latency of rearing in the corner test (Figure 1a and Table 1), with genotype (G **, $p < 0.01$), sex (S **, $p < 0.01$) and genotype per sex interaction effects (G × S *, $p < 0.05$) and male 3xTg-AD mice exhibiting statistically significant higher latencies than all the other groups (Figure 1a, post hoc, * and +, both $p < 0.05$); (2) the incidence of bizarre behaviors in the open-field test, with genotype (G ***, $p < 0.001$), sex (S **, $p < 0.01$) and genotype-by-sex (G × S **, $p < 0.01$) interaction effects, with male 3xTg-AD mice exhibiting statistically significant higher incidence than all the other groups (Figure 1a, post hoc, *** $p < 0.001$ and ++ $p < 0.01$).

3.2. Changes in Physical Condition, Organometrics, and the Endocrine System Are Sex-Dependent and Observable at 4 Months of Age in Male and Female 3xTg-AD Mice

The weight of animals, as well as the size (weight in mg) and relative size (% vs. body weight) of peripheral immunoendocrine organs, thymus, spleen, and adrenal glands, were recorded before the analysis of peripheral immune functions and the assessment of corticosterone levels. The results (Table 2) confirmed sexual dimorphism in body weight, with males being heavier than females (S ***, $p < 0.001$; $p < 0.05$ vs. respective female groups). Additionally, the overweight phenotype described for 3xTg-AD mice [16,26] was already present at this age (G ***, $p < 0.001$, $p < 0.05$ vs. respective NTg groups) and was attributed to a higher relative weight of white adipose tissue (WAT) (genotype and sex effects, both *** $p < 0.001$, $p < 0.05$ vs. respective NTg groups). Genotype differences were also observed in the relative weight of immunological organs, with a lower relative weight of thymus and a higher relative weight of spleen in 3xTg-AD mice (genotype effect, both G ***, $p < 0.001$; spleen, * $p < 0.05$ vs. respective NTg groups). The effect of sex was also observed in the weight of these organs, with the thymus and spleen being smaller in male than female mice (both, S **, $p < 0.01$).

Table 2. Physical condition, organometrics, and endocrine system in 4-month-old female and male NTg and 3xTg-AD mice.

	NTg		3xTg-AD		Factor Analysis G, Genotype S, Sex
	Females (n = 11)	**Males (n = 9)**	**Females (n = 8)**	**Males (n = 10)**	
Physical condition					
Body Weight (g)	21.7 ± 1.00	26.7 ± 0.50 +	26.3 ± 0.60 *	34.5 ± 0.90 * +	G ***, S ***, n.s.
% WAT in body weight	1.01 ± 0.06	0.80 ± 0.03	1.39 ± 0.04 *	1.22 ± 0.14 *	G ***, S ***, n.s.
Peripheral immune system					
% Thymus in body weight	0.18 ± 0.06	0.12 ± 0.01	0.15 ± 0.00	0.10 ± 0.00	G ***, S **, n.s.
% Spleen in body weight	0.38 ± 0.01	0.32 ± 0.01	0.52 ± 0.02 *	0.45 ± 0.07 *	G ***, S **, n.s.
Endocrine system					
Adrenal glands (mg)	8.2 ± 0.2	7.40 ± 0.5	7.3 ± 0.2	9.4 ± 0.6	n.s., n.s., G × S **
Plasma corticosterone (ng/mL)	35.5 ± 8.3	28.9 ± 7.2	43.3 ± 5.7	42.6 ± 7.8	n.s., n.s., n.s.

Results are the mean ± SEM of 8–11 animals. Statistics: Factor analysis: ** $p < 0.01$, and *** $p < 0.001$ vs. NTg (G, genotype effects), female mice (S, sex effects), or genotype × sex effects (G × S); n.s. non-statistically significant differences. Post hoc analysis: * $p < 0.05$ vs. NTg group with the same sex; + $p < 0.05$ vs. female group with the same genotype. NTg: non-transgenic mice; 3xTg-AD: triple transgenic mice for Alzheimer's disease. WAT: white adipose tissue.

At the endocrine level, a statistically significant genotype-by-sex effect (G × S **, $p < 0.01$) was found on the weight of adrenal glands, indicating a higher weight of this endocrine gland in male 3xTg-AD mice. A slight trend of higher plasma corticosterone concentrations in 3xTg-AD mice was observed, although it did not reach statistical significance ($p > 0.05$).

3.3. An Impairment of the Immune Functions Is Presented in 4-Month-Old Female and Male 3xTg-AD Mice

Several immune function parameters were studied in splenic and thymic leukocytes from female and male 3xTg-AD and NTg mice. The results are shown in Figures 2–5 and Tables 3 and 4. In general, at 4 months of age, 3xTg-AD mice showed an impairment of the immune functions in their splenic and thymic leukocytes.

Regarding chemotaxis (Figure 2a,b), our results showed that female and male 3xTg-AD mice had lower chemotactic index values in their spleen (Figure 2a, $p < 0.05$ and $p < 0.001$ in females and males, respectively) and thymus (Figure 2b, $p < 0.01$ and $p < 0.001$ in females and males, respectively) leukocytes than those observed in gender-matched NTg mice. Regarding sex differences, the lower values for chemotaxis observed in leukocytes of 3xTg-AD mice were more pronounced in males than in females ($p < 0.001$). By contrast, male NTg mice showed a higher chemotaxis index in their splenic leukocytes than NTg female mice ($p < 0.05$), whereas no gender differences were observed in thymic lymphocytes.

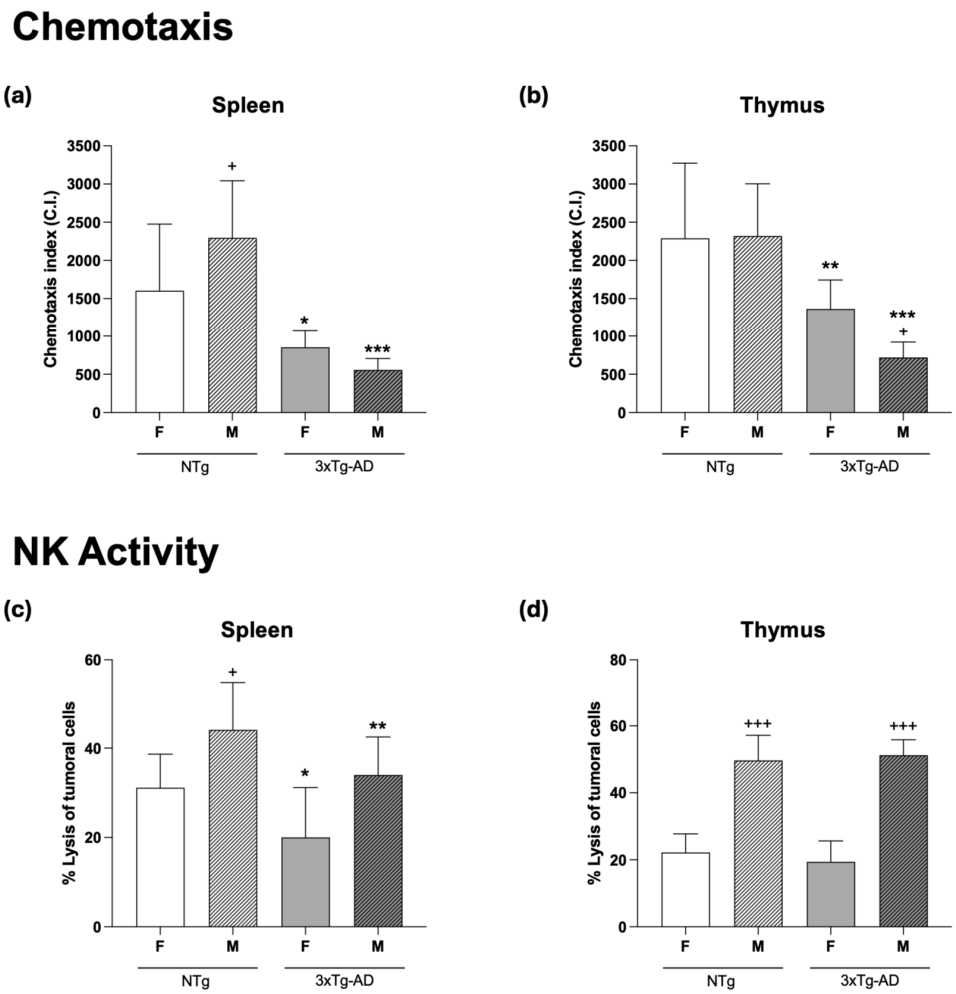

Figure 2. Immune function of 4-month-old female (F) and male (M) non-transgenic (NTg) and triple transgenic for Alzheimer's Disease (3xTg-AD) mice. Chemotactic index: (**a**) Spleen and (**b**) thymus leukocytes; Natural killer (NK) cell activity (% lysis of tumor cells): Spleen (**c**) and thymus (**d**) leukocytes. Each column represents the mean ± SEM of 8–11 values corresponding to the same number of subjects (NTg mice: 11 females, 9 males; 3xTg-AD mice: 8 females, 10 males). Each value is the mean of duplicate assays. Statistics: * $p < 0.05$, ** $p < 0.01$, *** $p < 0.001$ vs. NTg group with the same sex; + $p < 0.05$, +++ $p < 0.001$ vs. female group with the same genotype.

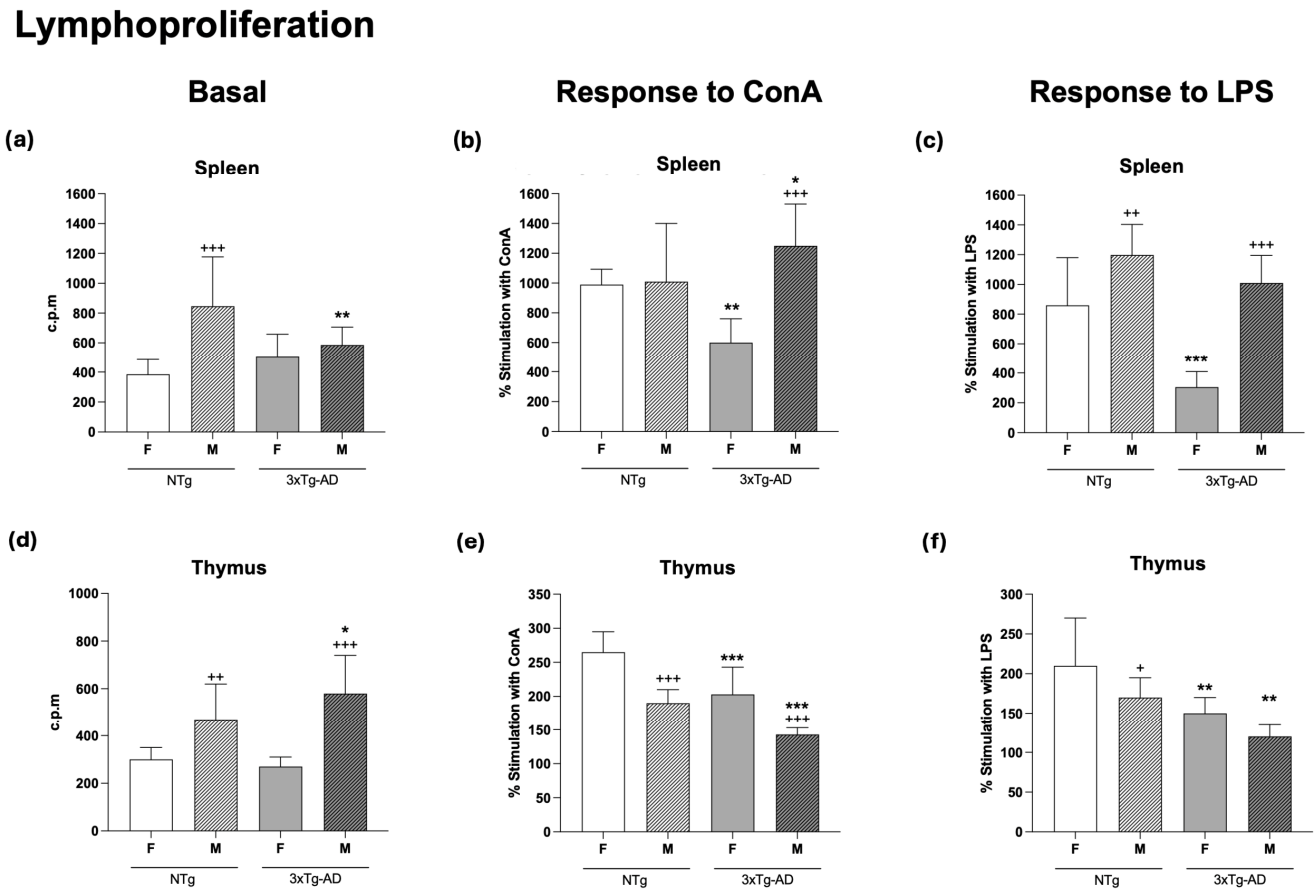

Figure 3. Proliferation of leukocytes of the (**a**–**c**) spleen and (**d**–**f**) thymus, in 4-month-old female (F) and male (M) non-transgenic (NTg) and triple transgenic for Alzheimer's Disease (3xTg-AD) mice. Basal (counts per minute; c.p.m.) and response to concanavalin A (Con A) and lipopolysaccharide (LPS) stimulated (% stimulation) conditions. Each column represents the mean ± SEM of 8–11 values corresponding to the same number of subjects (NTg mice: 11 females, 9 males; 3xTg-AD mice: 8 females, 10 males). Each value is the mean of triplicate assays. Statistics: * $p < 0.05$, ** $p < 0.01$, *** $p < 0.001$ vs. NTg group with the same sex; + $p < 0.05$, ++ $p < 0.01$, +++ $p < 0.001$ vs. female group with the same genotype.

An early impairment of NK cytotoxic activity (Figure 2) was also observed for spleen cells from female ($p < 0.05$) and male ($p < 0.01$) 3xTg-AD mice compared to gender-matched NTg mice (Figure 2c), whereas no statistical differences in NK activity were found in thymus lymphocytes between both groups of mice (Figure 2d). Regarding gender differences, both male NTg and 3xTg-AD mice exhibited higher NK activity in their splenic ($p < 0.05$, in NTg) and thymic ($p < 0.001$) leukocytes compared to female mice.

With respect to basal proliferation (Figure 3a,d), which is what takes place in the absence of a proliferative stimulus, there was a significantly lower value ($p < 0.01$) in spleen cells from male 3xTg-AD mice as compared to male NTg mice, while no differences between 3xTg-AD and NTg female mice were observed (Figure 3a). Moreover, no statistical differences were found in basal proliferation of thymus lymphocytes between 3xTg-AD and NTg mice (Figure 3d). Interestingly, in both splenic and thymic leukocytes, male NTg mice showed higher basal proliferation ($p < 0.001$ in spleen; $p < 0.01$ in thymus) than female NTg mice. Similar results were also observed in thymic cells of male 3xTg-AD ($p < 0.001$) compared to female 3xTg-AD mice (Figure 3d).

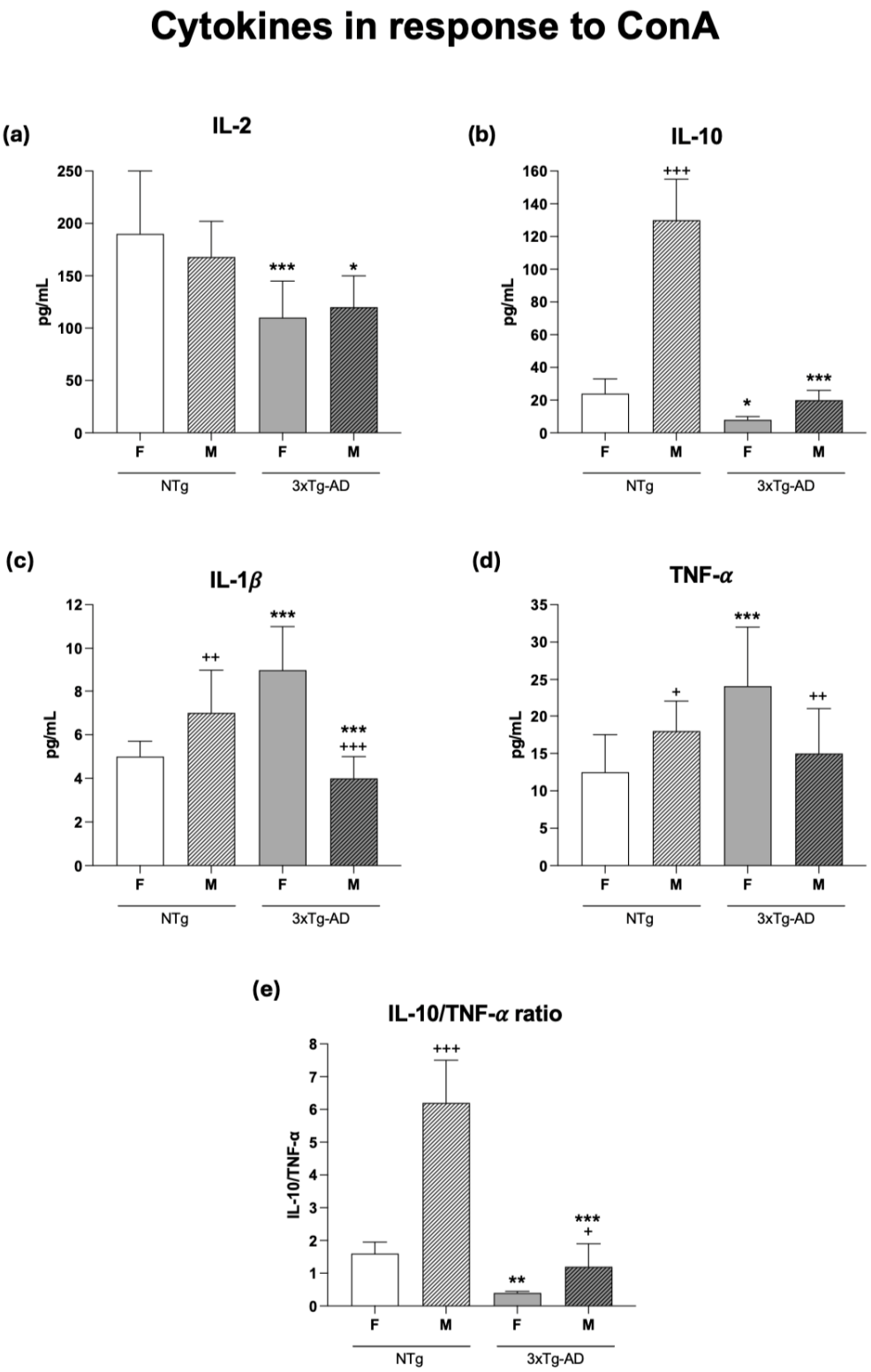

Figure 4. Concentrations of (**a**) IL-2, (**b**) IL-10, (**c**) IL-1β, and (**d**) TNF-α (pg/mL) and (**e**) IL-10/TNF-α ratio in supernatants of cultures of spleen leukocytes in response to concanavaline A (Con A) in 4-month-old female (F) and male (M) non-transgenic (NTg) and triple transgenic for Alzheimer's Disease (3xTg-AD) mice. Each column represents the mean ± SEM of 8–11 values corresponding to the same number of subjects (NTg mice: 11 females, 9 males; 3xTg-AD mice: 8 females, 10 males). Each value is the mean of duplicate assays. Statistics: * $p < 0.05$, ** $p < 0.01$, *** $p < 0.001$ vs. NTg group with the same sex; + $p < 0.05$, ++ $p < 0.01$, +++ $p < 0.001$ vs. female group with the same genotype.

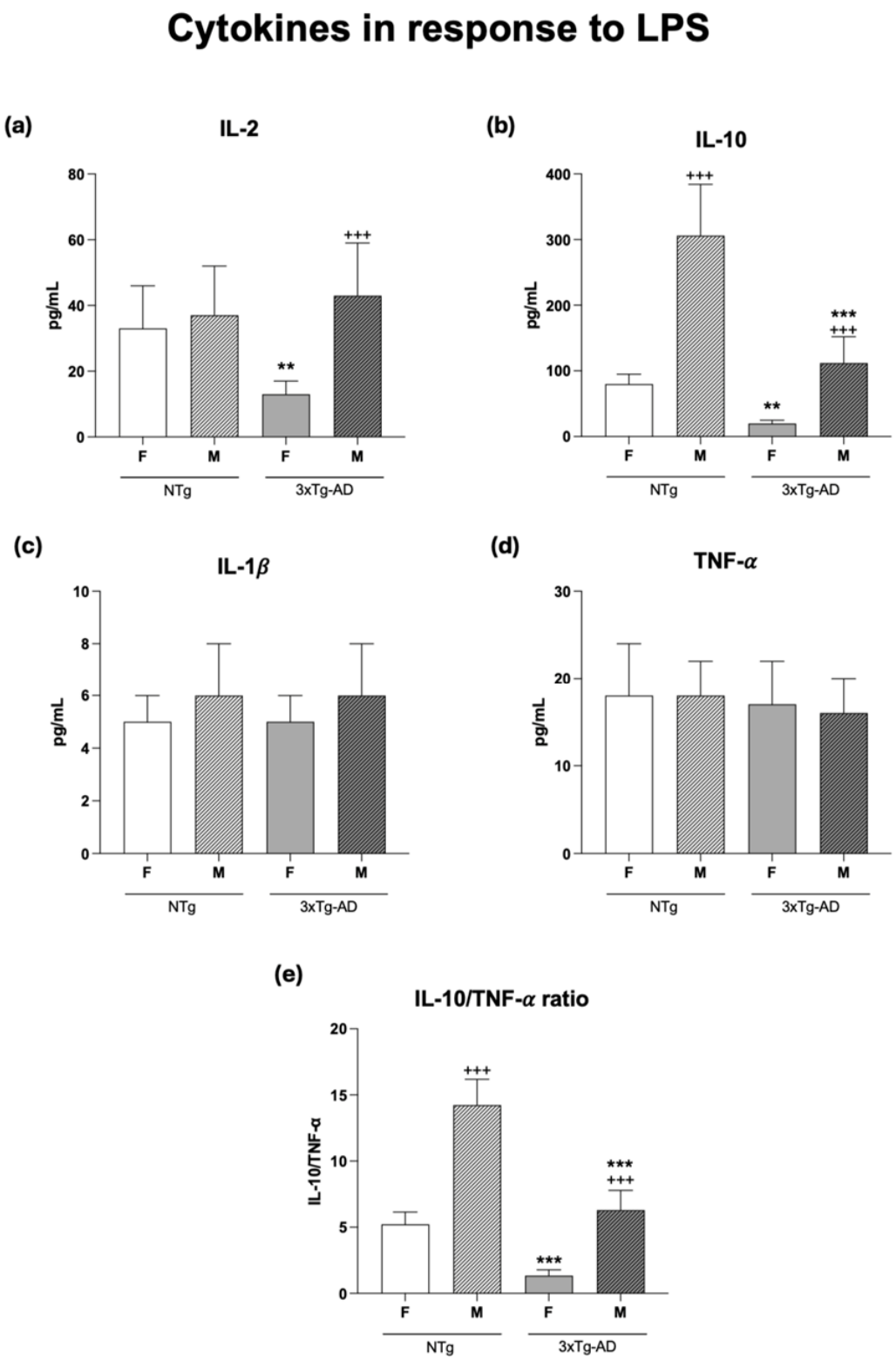

Figure 5. Concentrations of (**a**) IL-2, (**b**) IL-10, (**c**) IL-1β, and (**d**) TNF-α (pg/mL) and (**e**) IL-10/TNF-α ratio in supernatants of cultures of spleen leukocytes in response to lipopolysaccharide (LPS) in 4-month-old female (F) and male (M) non-transgenic (NTg) and triple transgenic for Alzheimer's Disease (3xTg-AD) mice. Each column represents the mean ± SEM of 8–11 values corresponding to the same number of subjects (NTg mice: 11 females, 9 males; 3xTg-AD mice: 8 females, 10 males). Each value is the mean of duplicate assays. Statistics: ** $p < 0.01$, *** $p < 0.001$ vs. NTg group with the same sex; +++ $p < 0.001$ vs. female group with the same genotype.

Table 3. Immune functions in spleen and thymus leukocytes in 4-month-old female and male 3xTg-AD and NTg mice.

	NTg		3xTg-AD		Factor Analysis G, Genotype Sex
	Females (*n* = 11)	**Males (*n* = 9)**	**Females (*n* = 8)**	**Males (*n* = 10)**	
Spleen leukocyte functions					
Chemotaxis index	1604.1 ± 871.75	2296.33 ± 747.47 +	852.82 ± 216.45 *	558.3 ± 147.71 ***	G ***, n.s., G × S *
NK activity (% Lysis)	31.15 ± 7.49	44.11 ± 10.59 +	20.04 ± 11.16 *	34.01 ± 8.5 **	G ***, n.s., G × S *
Lymphoproliferation Basal (c.p.m.)	385.02 ± 100.13	847.1 ± 330.06 +++	503.07 ± 155.03	585.2 ± 120.21 **	n.s., S ***, G × S **
Response to Con A (%)	991.04 ± 103.43	1012.23 ± 390.07	603.29 ± 160.3 **	1251.26 ± 280.6 * +++	n.s., S ***, G × S ***
Response to LPS (%)	863.27 ± 320.31	1198.09 ± 205.15 ++	305.33 ± 104.5 ***	1010.11 ± 185.04 +++	G ***, S ***, G × S *
Thymus leukocyte functions					
Chemotaxis index	2290.4 ± 983.4	2321.4 ± 682.9	1366.18 ± 379.1 **	720.6 ± 201.4 *** +	G ***, n.s., n.s.
NK activity (% Lysis)	22.19 ± 5.55	49.66 ± 7.51 +++	19.4 ± 6.25	51.22 ± 4.61 +++	n.s., S ***, n.s.
Lymphoproliferation Basal (c.p.m.)	302.52 ± 50.12	468.3 ± 150.55 ++	271.63 ± 40.39	582.23 ± 160.2 * +++	n.s., S ***, n.s.
Response to Con A (%)	265.51 ± 31.07	191.24 ± 19.8 +++	203.12 ± 40.03 ***	143.1 ± 10.18 *** +++	G ***, S ***, n.s.
Response to LPS (%)	210.3 ± 60.02	172.43 ± 25.33 +	149.89 ± 20.05 **	121.26 ± 15.37 **	G ***, S **, n.s.

Results are the mean ± SEM of 8–11 animals. Statistics: Factor analysis: * $p < 0.05$, ** $p < 0.01$, and *** $p < 0.001$ vs. NTg (G, genotype effects), or female mice (S, sex effects), or in the comparison to genotype × sex effects (G × S); n.s. non-statistical differences. Post hoc analysis: * $p < 0.05$, ** $p < 0.01$, *** $p < 0.001$ vs. NTg group with the same sex; + $p < 0.05$, ++ $p < 0.01$, +++ $p < 0.001$ vs. female group with the same genotype. NTg: non-transgenic mice; 3xTg-AD: triple transgenic mice for Alzheimer's disease. NK: natural killer; Con A: concanavaline A; LPS: lipopolysaccharide; c.p.m.: counts per minute.

Table 4. Concentrations of IL-2, IL-10, IL-1β, TNF-α, and TNF-α/IL-10 ratio in supernatants of cultures of splenic leukocytes in response to concanavaline A and lipopolysaccharide (LPS) from 4-month-old female (F) and male (M) non-transgenic (NTg) and triple transgenic Alzheimer's Disease (3xTgAD) mice.

	NTg		3xTg-AD		Factor Analysis G, Genotype S, Sex
	Females (*n* = 11)	**Males (*n* = 9)**	**Females (*n* = 8)**	**Males (*n* = 10)**	
Cytokine concentration in response to Concanavaline A					
IL-2 (pg/mL)	190 ± 60	168 ± 34	110 ± 35 ***	120 ± 30 *	G ***, n.s., n.s.
IL-10 (pg/mL)	24 ± 9	130 ± 25 +++	8 ± 2 *	20 ± 6 ***	G ***, S ***, G × S ***
IL-1β (pg/mL)	5 ± 0.7	7 ± 2 ++	9 ± 2 ***	4 ± 1 *** +++	n.s., S **, G × S ***
TNF-α (pg/mL)	12.5 ± 5	18 ± 4 +	24 ± 8 ***	15 ± 6 ++	G *, n.s., G × S ***
IL-10/TNF-α ratio	1.6 ± 0.35	6.2 ± 1.3 +++	0.4 ± 0.05 **	1.2 ± 0.7 *** +	G ***, S ***, G × S ***
IL-10/IL-2 ratio	0.13 ± 0.09	0.77 ± 0.07 +++	0.07 ± 0.04	0.16 ± 0.07 ***	G ***, S ***, G × S ***
IL-10/IL-1β ratio	4.8 ± 0.08	18.57 ± 1.08 +++	0.89 ± 0.05 ***	5 ± 0.17 *** +++	G ***, S ***, G × S ***
Cytokine concentration in response to Lipopolysaccharide					
IL-2 (pg/mL)	33 ± 13	37 ± 15	13 ± 4 **	43 ± 16 +++	n.s., S ***, G × S ***.
IL-10 (pg/mL)	80 ± 15	306 ± 78 +++	20 ± 5 **	112 ± 40 *** +++	G ***, S ***, G × S ***
IL-1β (pg/mL)	5 ± 1	6 ± 2	5 ± 1	6 ± 2	n.s., n.s., n.s.
TNF-α (pg/mL)	18 ± 6	18 ± 4	17 ± 5	16 ± 4	n.s., n.s., n.s.
IL-10/TNF-α ratio	5.23 ± 0.92	14.24 ± 1.95 +++	1.34 ± 0.44 ***	6.30 ± 1.49 *** +++	G ***, S ***, G × S ***
IL-10/IL-2 ratio	2.42 ± 1.15	8.27 ± 3.2 +++	1.54 ± 0.75	2.6 ± 1.35 ***	G ***, S **, G × S ***
IL-10/IL-1β ratio	16 ± 3.12	51 ± 10.02 +++	4 ± 1.07 *	18.67 ± 4.05 ***	G ***, S ***, G × S ***

Results are the mean ± SEM of 8–11 animals. Statistics: Factor analysis: * $p < 0.05$, ** $p < 0.01$, and *** $p < 0.001$ vs. NTg (G, genotype effects), or female mice (S, sex effects), or in the comparison to genotype × sex effects (G × S); n.s. non-statistical differences. Post hoc analysis: * $p < 0.05$, ** $p < 0.01$, *** $p < 0.001$ vs. NTg group with the same sex; + $p < 0.05$, ++ $p < 0.01$, +++ $p < 0.001$ vs. female group with the same genotype. NTg: non-transgenic mice; 3xTg-AD: triple transgenic mice for Alzheimer's disease.

The results for lymphoproliferation after incubation with the mitogens Con A (Figure 3b,e) and LPS (Figure 3c,f), which are specific for B and T lymphocytes, respectively, showed an impairment of this function in 3xTg-AD mice. In fact, significantly lower LPS-proliferative responses in spleen cells were observed in 4-month-old female (Figure 3c, $p < 0.001$) and in thymic cells of female and male (Figure 3f, $p < 0.001$) 3xTg-AD mice than in NTg mice. With Con A, in the case of splenic leukocytes, these lower values for proliferative response were only observed in female 3xTg-AD mice (Figure 3b, $p < 0.01$), but in thymic leukocytes in both female and male mice (Figure 3e, $p < 0.001$). Interestingly, regarding gender differences, male NTg mice showed higher ($p < 0.01$) and lower ($p < 0.05$) LPS proliferation percentage values in splenic and thymic leukocytes, respectively, than those observed in female animals. In the case of Con A-proliferative percentage, male NTg mice showed lower ($p < 0.001$) values in thymic cells. In male 3xTg-AD mice, Con A- and LPS-proliferative percentages of spleen leukocytes were higher ($p < 0.001$) than in females, but in thymic cells, these 3xTg-AD males showed lower ($p < 0.001$) values in Con A-proliferation than females.

Cytokines are major mediators of the complex interactions among immune cells, being responsible for the development and resolution of the immune response. For this reason, we analyzed the concentrations of several cytokines, including IL-2, IL-10, IL-1β, and TNF-α, secreted ex vivo by splenic leukocytes cultured for 48 h under conditions stimulated by Con A and LPS. In general, the results of our study showed that the release of these cytokines suffers impairments in 3xTg-AD mice, especially in females. Thus, as shown in Figures 4 and 5 and Table 4, under Con A- and LPS-stimulated conditions, lower concentrations of IL-2 and IL-10 were observed in female (Figure 4a,b, Con A, $p < 0.001$ and $p < 0.05$, respectively; Figure 5a,b, LPS, $p < 0.01$ for both) and male (Figure 4a,b, Con A, $p < 0.05$ and $p < 0.001$, respectively; Figure 5b, LPS, $p < 0.001$ in IL-10) 3xTg-AD mice in comparison to gender-matched NTg mice. Furthermore, under Con A-stimulated conditions, this was also accompanied by higher ($p < 0.001$) release of IL-1β and TNF-α only in females 3xTg-AD (Figure 4b,d, respectively). However, no differences were observed in these cytokines under stimulation with LPS (Figure 5b,d, respectively). Regarding gender differences, male NTg mice showed higher IL-10, IL-1β, TNF-α and concentrations ($p < 0.001$, $p < 0.01$, $p < 0.05$, respectively) in Con A presence (Figure 4b,c,d, respectively) and higher IL-10 ($p < 0.001$) with LPS stimulation (Figure 5b). However, male 3xTg-AD mice showed lower IL-1β and TNF-α concentrations under Con A-stimulated conditions (Figure 4c,d, $p < 0.001$ and $p < 0.01$, respectively) and higher IL-2 and IL-10 concentrations with LPS (Figure 5a,b, $p < 0.001$) than those observed in female 3xTg-AD mice.

The IL-10/TNF-α ratio under Con A-stimulated conditions (Figure 4d) showed lower values in female and male 3xTg-AD mice ($p < 0.01$ and $p < 0.001$, respectively) compared to their corresponding gender-matched NTg. Similarly, with LPS stimulation (Figure 5d) both female and male 3xTg-AD mice showed lower values ($p < 0.001$) than those in the corresponding NTg mice. Moreover, under Con-A and LPS stimulation, both male NTg ($p < 0.001$) and 3xTg-AD ($p < 0.05$ with Con A and $p < 0.001$ with LPS) mice presented a higher IL-10/TNF-α ratio than females (Figures 4d and 5d, respectively).

In addition, it was observed that for the IL-10/IL-2 and IL-10/IL-1β ratios, 3xTg-AD animals showed lower values both in Con A (Table 4, $p < 0.001$ for IL-10/IL-2 in males, and $p < 0.001$ for IL-10/IL-1β in females and males) and LPS stimulation (Table 4, $p < 0.001$ for IL-10/IL-2 in males, and $p < 0.05$, $p < 0.001$ for IL-10/IL-1β in females and males, respectively) compared to NTg animals. Regarding sex differences, NTg males showed higher IL-10/IL-2 and IL-10/IL-1β ratios in both Con A and LPS stimulation ($p < 0.001$) than NTg females. Meanwhile, 3xTgAD males showed a higher IL-10/IL-1β ratio in response to Con A (Table 5, $p < 0.001$) than 3xTgAD females.

3.4. Oxidative Stress Is Present in the Spleen of 4-Month-Old Female and Male 3xTg-AD Mice

As shown in Figure 6, 3xTg-AD mice exhibited higher values for oxidative stress markers at 4 months of age, particularly in male mice, compared to NTg animals. In fact, the values for the antioxidant enzymes such as GPx and GR activities (Figure 6a,b), as well as for the GSH concentrations (Figure 6c), were lower in 4-month-old female (GPx: $p < 0.01$; GR: $p < 0.05$; GSH: $p < 0.001$) and male (GPx: $p < 0.01$; GR and GSH: $p < 0.001$) 3xTg-AD mice than in NTg mice. Moreover, higher values for the pro-oxidant XO activity were found in female ($p < 0.01$) and male ($p < 0.001$) 3xTg-AD mice in comparison to NTg animals (Figure 6d). Finally, although the oxidative stress was more marked in male NTg mice, with lower values for GPx activity ($p < 0.05$) and GSH concentration ($p < 0.001$) than in female animals, in 3xAD-Tg mice, no statistical differences were observed in relation to sex.

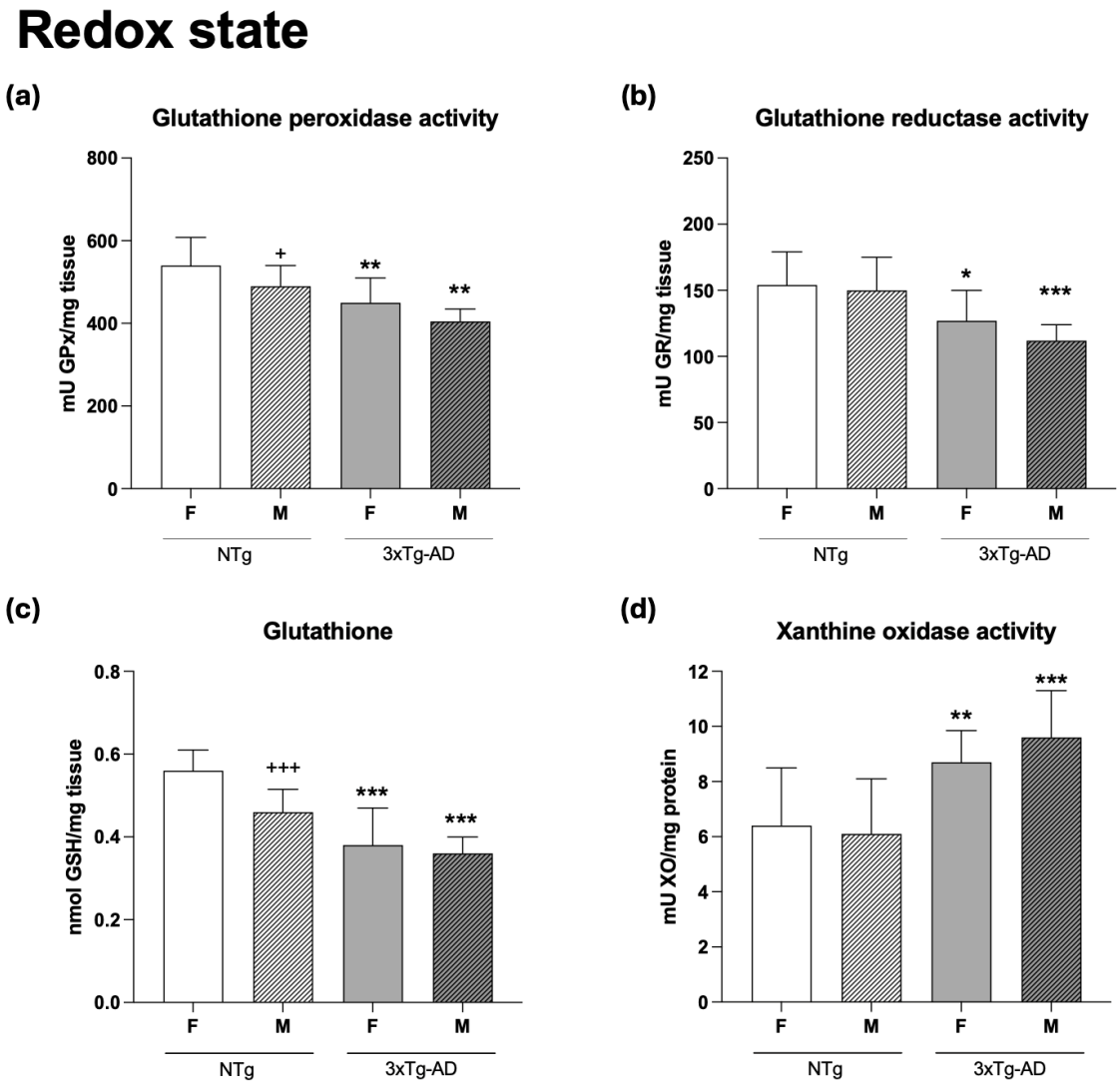

Figure 6. Redox state in homogenates of spleens from 4-month-old female (F) and male (M) non-transgenic (NTg) and triple transgenic for Alzheimer's Disease (3xTg-AD) mice. Glutathione peroxidase (GPx) activity (**a**), glutathione reductase (GR) activity (**b**), total reduced glutathione (GSH) concentrations (**c**), and xanthine oxidase (XO) activity (**d**). Each column represents the mean ± SEM of 8–11 values corresponding to the same number of subjects (NTg mice: 11 females, 9 males; 3xTg-AD mice: 8 females, 10 males). Each value is the mean of duplicate assays. Statistics: * $p < 0.05$, ** $p < 0.01$, *** $p < 0.001$ vs. NTg group with the same sex; + $p < 0.05$, +++ $p < 0.001$ vs. female group with the same genotype.

Table 5. Redox state in homogenates of spleens from 4-month-old female (F) and male (M) non-transgenic (NTg) and triple transgenic Alzheimer's Disease (3xTgAD) mice.

	NTg		3xTg-AD		Factor Analysis G, Genotype S, Sex
	Females (n = 11)	**Males (n = 9)**	**Females (n = 8)**	**Males (n = 10)**	
Glutathione peroxidase activity (mU GPx/mg tissue)	540 ± 68	490 ± 50 +	450 ± 60 **	405 ± 30 **	G ***, S *, n.s.
Glutathione reductase activity (mU GR/mg tissue)	154 ± 25	150 ± 25	127 ± 23 *	112 ± 12 ***	G ***, n.s., n.s.
Total reduced glutathione (nmol GSH/mg tissue)	0.56 ± 0.05	0.46 ± 0.05 +++	0.38 ± 0.09 ***	0.36 ± 0.04 ***	G ***, S **, G × S *
Xanthine oxidase activity (mU XO/mg tissue)	6.4 ± 2.1	6.1 ± 2	8.7 ± 1.15 **	9.6 ± 1.7 ***	G ***, n.s., n.s.

Results are the mean ± SEM of 8–11 animals. Statistics: Factor analysis: * $p < 0.05$, ** $p < 0.01$, and *** $p < 0.001$ vs. NTg (G, genotype effects), or female mice (S, sex effects), or in the comparison to genotype × sex effects (G × S); n.s. non-statistical differences. Post hoc analysis: * $p < 0.05$, ** $p < 0.01$, *** $p < 0.001$ vs. NTg group with the same sex; + $p < 0.05$, +++ $p < 0.001$ vs. female group with the same genotype. NTg: non-transgenic mice; 3xTg-AD: triple transgenic mice for Alzheimer's disease.

4. Discussion

According to our knowledge, this study is the first to conduct an integrative analysis of male and female 3xTg-AD mice at 4 months of age, when only intraneuronal immunoreactivity to beta-amyloid can be detected, and shows that their prodromal behavioral profile aligns with the first alterations in several components of the neuroimmunoendocrine network and redox state, proving the premature aging situation of these animals. Moreover, the present work is also the first to show an early hypertrophy of adrenal glands in male 3xTg-AD mice, while changes in corticosterone did not yet reach statistically significant differences.

4.1. Prodromal Behavioral Profile

In order to study the underlying derangement of the neuroimmunoendocrine system in males and females, we first verified their prodromal status. Thus, we determined the level of behavioral disturbances of 3xTg-AD animals at 4 months of age, as compared with sex- and age-matched NTg mice. This allowed us to provide further evidence on the early alteration of the different components of immune-endocrine function that align with their behavioral prodromal profile and to do so in both sexes.

4.1.1. Characteristics of Early BPSD-like Profile

At the behavioral level, the results of the present study show that, at 4 months of age, when early signs of behavioral and psychological symptoms of dementia (BDSP)-like alterations are observed in the 3xTg-AD mice, as characterized by our laboratory [26], a higher level of neophobia was measured by longer latency and lower number of rearings in the corner test. This was confirmed by changes in coping with stress strategies in the open-field test and T-maze.

This mouse model has provided evidence for the pathogenic role of intraneuronal Aβ in AD [26], and has shown how this early event relates to neuropathological aspects such as the affectation of the basolateral amygdala and the early appearance of BPSD-like symptoms [27]. These early BPSD-like symptoms are mostly related to emotionality, stress coping strategies, and exploratory behaviors, resembling those observed in patients at

the pre-clinical stages of the disease [57]. At all pre-pathological stages, disinhibitory behavior and a lack of ability to cope with mild stressors, such as novelty, are common features of the 3xTg-AD behavioral phenotype [58] and worsen with the progression of the disease [18,23]. Thus, these results resemble the stronger behavioral impairment in 3xTg-AD mice at advanced stages of disease [31] and indicate that they are present already at prodromal stages of disease.

In all these tests, genotype was the predominant factor to explain the consistent delay in the ethogram, that is, all the latencies of the behavioral events exhibited by both sexes of 3xTg-AD mice (initial freezing, thigmotaxis, vertical exploratory activity, and self-grooming behavior) and the consequent reduction in exploratory activity developed during the test as compared to NTg mice. Interestingly, several quantitative measures for exploratory efficiency in the T-maze indicated that they were, in fact, the result of qualitative differences in the behavioral patterns developed. Thus, both genotypes invested the same amount of time to complete the test, but this time corresponded to two different behavioral patterns, as evidenced by the ratio of time spent in the different arms and the number of errors. The poor ability to confront the test (higher latency to reach the intersection) exhibited by 3xTg-AD mice was followed by a short exploratory activity of the horizontal arms. In contrast, in the NTg mice, the ratio indicated a preference for exploring the two horizontal arms, which is the basis of the spontaneous alternation typical of animals' behavior in this maze [59]. Therefore, it is essential to note that the lack of differences in total exploration time does not align with the qualitative differences in the behavioral profile, rendering this time variable a non-specific measure and necessitating caution when studied alone. In addition, it is interesting to note that the mean time to reach the intersection in the T-maze is a behavioral paradigm related to worse immunosenescence and reduced survival in prematurely aging mice (PAM) as compared to non-prematurely aging mice (NPAM) [8,43].

The higher number of defecation boli and the presence of urination in 3xTg-AD mice are considered to indicate changes in their emotionality [23]. We have previously reported such changes at 6, 7, 12, and 18 months of age, but not before, during young adulthood (2 months of age), nor at the early onset of the symptoms of the disease (6 months of age) [23,51]. In the present work, we found statistically significant differences in defecation between genotypes and sexes, which were primarily due to a higher number in NTg females. These post hoc differences may indicate that female NTg mice are more sensitive to exhibiting the higher emotionality of female sex than 3xTg-AD mice at this age [51].

4.1.2. Specific Sex-Per Genotype-Effects

As described above, some specific sex and genotype effects could be observed. Thus, on the one hand, male 3xTg-AD mice were more prone to exhibit BPSD-like alterations, such as neophobia in the corner test and bizarre behaviors in the open-field test. On the other hand, female 3xTg-AD mice were the ones to exhibit the most intense initial freezing behavior in the open-field test and the highest delay to reach the criteria (intersection) in the T-maze, which in both cases are known to be indicative of higher fearfulness and/or poor coping with stress strategies [39]. Other variables, such as the number of errors, also indicate differences between genotypes by sex in this respect.

Overall, the behavioral data indicate BDSP-like alterations in 3xTg-AD mice at 4 months of age, during the early stages of the disease, and highlight the relevance of genotype effects underlying these alterations. In all the tests, horizontal and vertical exploratory activities were lower than in controls, although differences only reached statistical significance in the vertical component, which is the one known to be more sensitive in detecting changes in exploratory activity [60].

4.2. Organometrics and Plasma Corticosterone

The overweight described for 3xTg-AD mice, especially in males [26], was already present at this age, and it could be due to a higher relative weight of white adipose tissue. The organometrics of peripheral immune organs are relevant to understanding physical variation and changes associated with disease [28,31,51]. Thus, in 3xTg-AD mice, we have reported that both total weight and relative weight of peripheral immunoendocrine organs such as thymus, spleen, and adrenal glands correlate with the sex-dependent impairment of the neuroimmunoendocrine network described at advanced stages of the disease, and even at 6 months of age [28,31,51]. The present work indicates that these changes can already be observed at early stages of the disease; however, immunological organs are more sensitive in exhibiting changes in their organometrics than the endocrine glands. Interestingly, the hypertrophy of the adrenal glands in male 3xTg-AD mice reached statistically significant values, while the plasma levels of corticosterone, a hormone very representative of the endocrine system state and related to stress response and the neuroimmunoendocrine system [42,56], just showed a slight trend. Since higher corticosterone levels have been reported in 3xTg-AD males at 15 months of age as compared to controls [31,61], the window of 4 months of age studied in the present work allowed observing, for the first time, the existence of a temporal derangement delay within the different homeostasis (neuro-immuno-endocrine) systems.

4.3. Immune Functions

The nervous and immune systems are intricately connected through bidirectional communication that regulates the function and homeostatic roles of both systems [62,63]. Thus, changes in one of these systems due to aging or pathological AD could influence the other, and vice versa. At the translational level, in the 3xTg-AD mice, an accelerated deterioration of the neuroimmune system has been reported at 15 months of age, which mimics advanced stages of Alzheimer's disease [17,19], especially in males, demonstrating the relevance of this system in the etiopathogenesis of AD and its relation with the shorter lifespan of males than that of females [31].

4.3.1. Early Innate and Adaptive Immunity Impairment

Immune system functions analyzed in leukocytes from the spleen and thymus included functions of innate immunity (chemotaxis and antitumoral natural killer activity) and of adaptive immunity (lymphoproliferation in response to Con A and LPS mitogens). The results provide evidence of the presence of the neuroimmune system impairment in 3xTg-AD mice already at early stages of the disease (4 months of age), in males and females. Thus, both sexes of 3xTg-AD mice exhibited a lower chemotactic index in spleen and thymus leukocytes compared to NTg mice, with a more pronounced effect in males. The natural killer activity against tumor cells was also lower in leukocytes from 3xTg-AD mice than in NTg animals, but these differences were only detectable in the spleen, and again, males were more affected. It is known that these two functions, representatives of innate immunity, exhibit age-related changes. In general, these changes are shown as lower values in these functions, which represent worse innate defense mechanisms [8,14,46,64].

On the other hand, a lower lymphoproliferative response to the mitogens Con A and LPS, a typical adaptive immune function, was shown in 3xTg-AD mice in comparison with NTg mice, in the spleen (only in females) and in the thymus (in both sexes). This lower proliferation, a characteristic of immunosenescence [8,65], in spleen leukocytes from females could be due, at least in part, to the lower capacity of these cells to release IL-2, a cytokine involved in this proliferative response [66].

These early altered functions in leukocytes from immune organs (spleen and thymus) agree with the results observed at 4 months of age in our previous longitudinal study of peritoneal immune cells performed in female 3xTg-AD mice [29,30]. However, whereas the innate functions of chemotaxis and NK activity were also lower in female 3xTgAD mice than in their NTg counterparts—similarly to the present results from immune organs, especially in the spleen—the proliferation of lymphocytes was higher in peritoneal leukocytes from 3xTg-AD mice than that from the female controls. These results show that in this animal model of AD, the differences with controls in the immune functions depend on the leukocyte location, at least in adaptive immunity. Nevertheless, in a model of prematurely aging mice (PAM) and lower lifespan than non-prematurely aging mice (NPAM), we reported that all these immune functions in the peritoneum of female PAM showed lower values than those in NPAM controls, and this had also happened already in young adult animals at 4 months of age [8,39]. Moreover, these premature alterations detected in the peritoneum were also observed in immune organs, such as the spleen and thymus, of these PAM [43]. Nevertheless, not all murine models involving premature aging show similar changes in immunosenescence in the different locations of the immune system. However, these findings underscore the immune system as not only a defense mechanism but also as a sensitive indicator of systemic aging and health state, as we previously proposed [67].

4.3.2. Unbalanced Anti-Inflammatory/Proinflammatory Cytokines

The pro- and anti-inflammatory cytokines released by spleen leukocytes showed differences depending on sex and the mitogen used. Thus, with Con A, a mitogen more specific to T lymphocytes [30], the concentrations of proinflammatory cytokines such as IL-1β and TNF-α in female 3xTg-AD mice were higher than in NTg females. However, in males, the concentrations of IL-1β released by cells from 3xTg-AD mice were lower than those from NTg mice, whereas no differences were found in TNF-α. Nevertheless, since the amounts of the anti-inflammatory cytokine, IL-10, were lower in 3xTg-AD mice of both sexes, the ratio IL-10/TNF-α—a good indicator of an appropriate balance of anti-inflammatory/pro-inflammatory cytokines and successful aging and longevity [30,68]—was also lower in both sexes of 3xTg-AD mice than in the sex-matched NTg animals, similarly as occurred with the other anti-inflammatory/pro-inflammatory cytokine ratios analyzed in response to Con A and also to LPS. Therefore, this loss of anti-inflammatory control, which could explain the incorrect immune response and the possible arrival of pro-inflammatory compounds in the brain, generating the neuroinflammation characteristic of these pathologies [7], appears to occur at an early age in these 3xTg-AD mice. Moreover, an inflammatory stress has also been reported, with a higher secretion of proinflammatory cytokines, such as IL-1β, and the ratios IL-1/IL-10 and IL-6/IL-10 in peritoneal leukocytes from 4-month-old 3xTg-AD females [30]. From the bench-to-bedside, this peripheral inflammation has been linked to AD initiation and progression in preclinical and clinical studies [7,40].

4.4. Redox-Inflammatory State

It is known that the presence of both oxidative and inflammatory stress, especially in immune cells, underlies aging and neurodegenerative processes [8,14,29]. In this sense, the longitudinal study of peritoneal immune cells in 3xTg-AD females showed that they have a premature oxidative stress status from 4 months of age [29,30]. This stress was characterized by lower concentrations of the endogenous antioxidant glutathione reduced (GSH), which is related to immune function [8], higher activity of XO, a pro-oxidant enzyme with dual roles in the immune system, acting as innate defense but contributing to inflammation-related pathology [69] and higher lipid oxidative damage compared to female NTg mice [29,30].

Sex differences in neuroimmunoendocrine communication and their involvement in longevity point to worse immune response and higher oxidative stress in males than in females, which explains their shorter lifespan [46]. However, these sex differences are strain- and age-dependent, being more evident in adult animals [46]. Thus, despite 15-month-old 3xTg-AD males showing lower concentrations of GSH than females, at least in spleen, a lack of genotype differences in the concentrations in lymphocytes of spleen and thymus of males and females, as compared with the corresponding values in NTg animals, was described [31]. Therefore, the present study was important to investigate the redox-inflammatory state of spleens in male and female 3xTg-AD mice at 4 months of age. The results showed an oxidative stress situation as compared to their NTg counterparts, with antioxidant defenses such as the activity of the antioxidant enzymes of the glutathione cycle GPx and GR, as well as the concentrations of GSH, being lower in male and female 3xTg-AD mice than in NTg mice. With respect to XO, the present study showed that the activity of XO in the spleen was higher in both sexes of 3xTg-AD mice, but male 3xTg-AD mice were the most affected. Interestingly, in a study in a high-risk AD human population, we have recently shown that elevated uric acid and urea levels were associated with poorer cognitive performance [70].

Although the use of transgenic mice to research translational strategies in AD has been found to be limited by several authors [71,72], 3xTg-AD mice have been proven useful in this context by many others [73–76]. The present study confirms the importance of neuroimmune communication and peripheral immunity in AD pathogenesis [13], also indicating that at this early stage of the disease, oxidative and inflammatory stresses are already present. Therefore, its translational value lies in identifying a very early preclinical window of opportunity for AD intervention, highlighting sex-specific and multi-systemic (behavioral, immune, and redox) biomarkers observed at 4 months of age. This fact, together with the premature immunosenescence, which is associated with oxidative-inflammatory stress [8,39], and also with the premature aging of several behavioral responses, confirms the premature aging of these 3xTg-AD mice and explains their shorter lifespan [30,31]. The present work also demonstrates the relevance of BPSD-like symptoms and the peripheral immune system functional and redox status as early indicators of disease onset, before cognitive deficits and alterations in plasmatic glucocorticoid levels can be detected.

Whereas amyloid accumulation is often faster in females, male 3xTg-AD mice show early signs of systemic autoimmunity and frailty (40% mortality) [25,27,31], making this animal model useful to study sex-specific progression. The lack of estrous cycle monitoring in females should be explicitly acknowledged as a limitation of the present study. However, it is significant that at 4 months of age, no sex differences have been described at the immunohistochemical level for intraneuronal βA and tau immunoreactivity at this age [25–27,61]. This reinforces the value of the findings for BPSD-like behaviors and the peripheral immune system as early indicators of the alterations during these prodromal stages of the disease.

Therefore, the evidence of a genotype- and sex-dependent time lag, where behavioral and immune alterations (i.e., splenic immune dysfunction, early adrenal hypertrophy in males) are present, while plasmatic corticosterone does not show statistically significant alterations, is relevant for understanding and targeting the homeostasis network derangement in AD.

In addition, since the results obtained in 3xTg-AD mice appear similar to those observed in human AD patients [14,32], a better understanding of each of these homeostatic systems and their interaction by means of an integrative approach that evaluates, in the same animals, immune functions and behavioral status encourages the development of new preventive and therapeutic strategies and the design of interventions targeting this

premature neuroimmune and redox-inflammation breakdown. In fact, treatment with an anti-TNFSF10 monoclonal antibody in 3xTg-AD mice restrains overshooting central and peripheral (spleen) inflammation by rebalancing the immune response, mitigating the progression of AD pathology in these animals [35]. Therefore, at the translational level, the present study could have implications for early detection and prevention, suggesting these prodromal peripherally accessible immune and redox markers as early tools to identify people at presymptomatic, prodromal, or mild cognitive impairment stages, and the opportunity of targeting this early dysfunction as an earlier and more effective intervention.

5. Conclusions

In the 3xTg-AD mice, the impairment of the neuroendocrine-immune network becomes apparent at the prodromal stage of AD (4 months old), with sex differences. We also demonstrate that the different regulatory systems involved in this network exhibit distinct sensitivities in responding to these changes. This study demonstrates the relevance of BPSD-like symptoms, peripheral immune cell functions, and redox and inflammatory states as early indicators of disease onset in this animal model, before cognitive deficits and statistically significant changes in plasma corticosterone can be detected. Thus, we propose these biomarkers, identified at prodromal stages in both male and female 3xTg-AD mice, as tools of interest at both a translational and clinical level. At the biological level, the characterization of these distinct temporal derangements is useful for a better design of new biomolecules and the assessment of preventive/treatment strategies and opportunities. At the clinical level, they could be useful for risk assessment, early diagnosis, evaluation of disease progression, and assessment of treatment effectiveness in clinical trials. In addition, the alterations in behavior and immunity, as well as the oxidative-inflammatory stress observed in 3xTg-AD mice at this young age, confirm the premature aging of these animals, explaining their lower longevity.

Author Contributions: Conceptualization, L.G.-L. and M.D.l.F.; methodology, L.G.-L., C.V. and R.M.; software, L.G.-L., C.V. and J.F.; formal analysis, L.G.-L., C.V., J.F. and S.Q.-P.; investigation, L.G.-L., C.V. and R.M.; data curation, L.G.-L. and C.V.; writing—original draft preparation, L.G.-L. and M.D.l.F.; writing—review and editing, L.G.-L., M.D.l.F. and J.F.; supervision, L.G.-L. and M.D.l.F.; project administration, L.G.-L. and M.D.l.F.; funding acquisition, L.G.-L. and M.D.l.F. All authors have read and agreed to the published version of the manuscript.

Funding: This research was funded by FIS ISC3 PI10/00283, RETICEF (Red de Envejecimiento y Fragilidad) ISC3 RD06/0013/0003, Research Group of Translational Behavioral Neuroscience UAB-GE-260408, and the Research Group of UCM-CM (ENEROINN 910379), Generalitat de Catalunya 2021 SGR-00529.

Institutional Review Board Statement: All the experiments were conducted in accordance with the Spanish legislation on "Protection of Animals Used for Experimental and Other Scientific Purposes" and the EU Directive (2010/63/EU) on this subject, and the Ethical Commission of the Universitat Autònoma de Barcelona (Protocol Number CEEAH/00759 3588/DMAH 9452, 8 March 2019).

Informed Consent Statement: Not applicable.

Data Availability Statement: Data will be available upon request to Lydia Giménez-Llort (lidia.gimenez@uab.cat).

Acknowledgments: We would like to thank Frank M. LaFerla (Department of Neurobiology and Behavior, University of California Irvine, CA, USA) for providing us with the progenitor animals.

Conflicts of Interest: The authors declare no conflicts of interest.

References

1. Knopman, D.S.; Amieva, H.; Petersen, R.C.; Chételat, G.; Holtzman, D.M.; Hyman, B.T.; Nixon, R.A.; Jones, D.T. Alzheimer Disease. *Nat. Rev. Dis. Primers* **2021**, *7*, 33. [CrossRef]
2. Feigin, V.L.; Vos, T.; Nichols, E.; Owolabi, M.O.; Carroll, W.M.; Dichgans, M.; Deuschl, G.; Parmar, P.; Brainin, M.; Murray, C. The Global Burden of Neurological Disorders: Translating Evidence into Policy. *Lancet Neurol.* **2020**, *19*, 255–265. [CrossRef] [PubMed]
3. Ferreira, D.; Wahlund, L.O.; Westman, E. The Heterogeneity within Alzheimer's Disease. *Aging* **2018**, *10*, 3058. [CrossRef]
4. Livingston, G.; Huntley, J.; Liu, K.Y.; Costafreda, S.G.; Selbæk, G.; Alladi, S.; Ames, D.; Banerjee, S.; Burns, A.; Brayne, C.; et al. Dementia prevention, intervention, and care: 2024 report of the Lancet standing Commission. *Lancet* **2024**, *404*, 572–628. [CrossRef]
5. Lomi, M.; Geraci, F.; Del Seppia, C.; Dolciotti, C.; Del Carratore, R.; Bongioanni, P. Biomarker profile in peripheral blood cells related to Alzheimer's disease. *Mol. Neurobiol.* **2025**, *62*, 8949–8964. [CrossRef] [PubMed]
6. Yasumo, F.; Watanabe, A.; Kimura, Y.; Yamauchi, Y.; Ogata, A.; Ikenuma, H.; Abe, J.; Minami, H.; Nihashi, T.; Yokoi, K.; et al. Plasma IL-6 levels as a biomarker for behavioral changes in Alzheimer's disease. *Neuroimmunomodulation* **2025**, *32*, 233–244. [CrossRef]
7. Malarte, M.L.; Chiotis, K.; Ioannou, K.; Rodriguez-Vieitez, E. Peripheral inflammation is associated with greater neuronal injury and lower episodic memory among late middle-aged adults. *J. Neurochem.* **2025**, *169*, e70222. [CrossRef]
8. De la Fuente, M.; Miquel, J. An update of the oxidation-inflammation theory of aging: The involvement of the immune system in oxi-inflamm-aging. *Curr. Pharm. Des.* **2009**, *15*, 3003–3026. [CrossRef]
9. McManus, R.M. The Role of Immunity in Alzheimer's Disease. *Adv. Biol.* **2022**, *6*, e2101166. [CrossRef]
10. Long, C.; Fritts, A.; Broadway, J.; Brawman-Mintzer, O.; Mintzer, J. Neuroinflammation: A Driving Force in the Onset and Progression of Alzheimer's Disease. *J. Clin. Med.* **2025**, *14*, 331. [CrossRef] [PubMed]
11. Heneka, M.T.; van der Flier, W.M.; Jessen, F.; Hoozemanns, J.; Thal, D.R.; Boche, D.; Brosseron, F.; Teunissen, C.; Zetterberg, H.; Jacobs, A.H.; et al. Neuroinflammation in Alzheimer disease. *Nat. Rev. Immunol.* **2025**, *25*, 321–352. [CrossRef] [PubMed]
12. Zang, X.; Chen, S.; Zhu, J.; Ma, J.; Zhai, Y. The Emerging Role of Central and Peripheral Immune Systems in Neurodegenerative Diseases. *Front. Aging Neurosci.* **2022**, *14*, 872134. [CrossRef]
13. Zhang, S.; Gao, Y.; Zhao, Y.; Huang, T.Y.; Zheng, Q.; Wang, X. Peripheral and central neuroimmune mechanisms in Alzheimer's disease pathogenesis. *Mol. Neurodegener.* **2025**, *20*, 22. [CrossRef]
14. Vida, C.; Martinez de Toda, I.; Garrido, A.; Carro, E.; Molina, J.A.; De la Fuente, M. Impairment of Several Immune Functions and Redox State in Blood Cells of Alzheimer's Disease Patients. Relevant Role of Neutrophils in Oxidative Stress. *Front. Immunol.* **2018**, *8*, 1974. [CrossRef]
15. Puzzo, D.; Gulisano, W.; Palmeri, A.; Arancio, O. Rodent Models for Alzheimer's Disease Drug Discovery. *Expert Opin. Drug Discov.* **2015**, *10*, 703–711. [CrossRef]
16. Sanchez-Varo, R.; Mejias-Ortega, M.; Fernandez-Valenzuela, J.J.; Nuñez-Diaz, C.; Caceres-Palomo, L.; Vegas-Gomez, L.; Sanchez-Mejias, E.; Trujillo-Estrada, L.; Garcia-Leon, J.A.; Moreno-Gonzalez, I.; et al. Transgenic Mouse Models of Alzheimer's Disease: An Integrative Analysis. *Int. J. Mol. Sci.* **2022**, *23*, 5404. [CrossRef]
17. Oddo, S.; Caccamo, A.; Shepherd, J.D.; Murphy, M.P.; Golde, T.E.; Kayed, R.; Metherate, R.; Mattson, M.P.; Akbari, Y.; LaFerla, F.M. Triple-transgenic model of Alzheimer's disease with plaques and tangles: Intracellular Abeta and synaptic dysfunction. *Neuron* **2003**, *39*, 409–421. [CrossRef]
18. Oddo, S.; Caccamo, A.; Kitazawa, M.; Tseng, B.P.; LaFerla, F.M. Amyloid deposition precedes tangle formation in a triple transgenic model of Alzheimer's disease. *Neurobiol. Aging* **2003**, *24*, 1063–1070. [CrossRef] [PubMed]
19. Oddo, S.; Caccamo, A.; Green, K.N.; Liang, K.; Tran, L.; Chen, Y.; Leslie, F.M.; LaFerla, F.M. Chronic nicotine administration exacerbates tau pathology in a transgenic model of Alzheimer's disease. *Proc. Natl. Acad. Sci. USA* **2005**, *102*, 3046–3051. [CrossRef] [PubMed]
20. Oddo, S.; Caccamo, A.; Tran, L.; Lambert, M.P.; Glabe, C.G.; Klein, W.L.; LaFerla, F.M. Temporal profile of amyloid-beta (Abeta) oligomerization in an in vivo model of Alzheimer's disease. A link between Abeta and tau pathology. *J. Biol. Chem.* **2006**, *281*, 1599–1604. [CrossRef] [PubMed]
21. Billings, L.M.; Oddo, S.; Green, K.N.; McGaugh, J.L.; LaFerla, F.M. Intraneuronal Abeta causes the onset of early Alzheimer's disease-related cognitive deficits in transgenic mice. *Neuron* **2005**, *45*, 675–688. [CrossRef] [PubMed]
22. Janelsins, M.C.; Mastrangelo, M.A.; Oddo, S.; LaFerla, F.M.; Federoff, H.J.; Bowers, W.J. Early correlation of microglial activation with enhanced tumor necrosis factor-alpha and monocyte chemoattractant protein-1 expression specifically within the entorhinal cortex of triple transgenic Alzheimer's disease mice. *J. Neuroinflammation* **2005**, *2*, 23. [CrossRef] [PubMed]
23. Kitazawa, M.; Oddo, S.; Yamasaki, T.R.; Green, K.N.; LaFerla, F.M. Lipopolysaccharide-induced inflammation exacerbates tau pathology by a cyclin-dependent kinase 5-mediated pathway in a transgenic model of Alzheimer's disease. *J. Neurosci.* **2005**, *25*, 8843–8853. [CrossRef] [PubMed]

24. Sterniczuk, R.; Antle, M.C.; Laferla, F.M.; Dyck, R.H. Characterization of the 3xTg-AD mouse model of Alzheimer's disease: Part 2. Behavioral and cognitive changes. *Brain Res.* **2010**, *1348*, 149–155. [CrossRef]
25. Belfiore, R.; Rodin, A.; Ferreira, E.; Velazquez, R.; Branca, C.; Caccamo, A.; Oddo, S. Temporal and regional progression of Alzheimer's disease-like pathology in 3xTg-AD mice. *Aging Cell* **2019**, *18*, e12873. [CrossRef]
26. Giménez-Llort, L.; Blázquez, G.; Cañete, T.; Johansson, B.; Oddo, S.; Tobeña, A.; LaFerla, F.M.; Fernández-Teruel, A. Modeling behavioral and neuronal symptoms of Alzheimer's disease in mice: A role for intraneuronal amyloid. *Neurosci. Biobehav. Rev.* **2007**, *31*, 125–147. [CrossRef]
27. Muntsant, A.; Castillo-Ruiz, M.D.M.; Giménez-Llort, L. Survival Bias, Non-Lineal Behavioral and Cortico-Limbic Neuropathological Signatures in 3xTg-AD Mice for Alzheimer's Disease from Premorbid to Advanced Stages and Compared to Normal Aging. *Int. J. Mol. Sci.* **2023**, *24*, 13796. [CrossRef]
28. Giménez-Llort, L.; Torres-Lista, V.; De la Fuente, M. Crosstalk between behavior and immune system during the prodromal stages of Alzheimer's disease. *Curr. Pharm. Des.* **2014**, *20*, 4723–4732. [CrossRef]
29. Maté, I.; Cruces, J.; Giménez-Llort, L.; De la Fuente, M. Function and redox state of peritoneal leukocytes as preclinical and prodromic markers in a longitudinal study of triple-transgenic mice for Alzheimer's disease. *J. Alzheimer's Dis.* **2015**, *43*, 213–226. [CrossRef]
30. Ceprián, N.; Martínez de Toda, I.; Maté, I.; Garrido, A.; Gimenez-Llort, L.; De la Fuente, M. Prodromic Inflammatory-Oxidative Stress in Peritoneal Leukocytes of Triple-Transgenic Mice for Alzheimer's Disease. *Int. J. Mol. Sci.* **2024**, *25*, 6976. [CrossRef]
31. Giménez-Llort, L.; Arranz, L.; Maté, I.; De la Fuente, M. Gender-specific neuroimmunoendocrine aging in a triple-transgenic 3xTg-AD mouse model for Alzheimer's disease and its relation with longevity. *Neuroimmunomodulation* **2008**, *15*, 331–343. [CrossRef]
32. St-Amour, I.; Bosoi, C.R.; Paré, I.; Ignatius Arokia Doss, P.M.; Rangachari, M.; Hébert, S.S.; Bazin, R.; Calon, F. Peripheral adaptive immunity of the triple transgenic mouse model of Alzheimer's disease. *J. Neuroinflammation* **2019**, *16*, 3. [CrossRef] [PubMed]
33. Yang, S.H.; Kim, J.; Lee, M.J.; Kim, Y. Abnormalities of plasma cytokines and spleen in senile APP/PS1/Tau transgenic mouse model. *Sci. Rep.* **2015**, *5*, 15703. [CrossRef]
34. Fraile-Ramos, J.; Reig-Vilallonga, J.; Giménez-Llort, L. Glomerular Hypertrophy and Splenic Red Pulp Degeneration Concurrent with Oxidative Stress in 3xTg-AD Mice Model for Alzheimer's Disease and Its Exacerbation with Sex and Social Isolation. *Int. J. Mol. Sci.* **2024**, *25*, 6112. [CrossRef]
35. Cantone, A.F.; Burgaletto, C.; Di Benedetto, G.; Gaudio, G.; Giallongo, C.; Caltabiano, R.; Broggi, G.; Bellanca, C.M.; Cantarella, G.; Bernardini, R. Rebalancing immune interactions within the brain-spleen axis mitigates neuroinflammation in an aging mouse model of Alzheimer's disease. *J. Neuroimmune Pharmacol.* **2025**, *20*, 15. [CrossRef]
36. Bai, R.; Guo, J.; Ye, X.Y.; Xie, Y.; Xie, T. Oxidative stress: The core pathogenesis and mechanism of Alzheimer's disease. *Ageing Res. Rev.* **2022**, *77*, 101619. [CrossRef] [PubMed]
37. Torres-Lista, V.; Parrado-Fernández, C.; Alvarez-Montón, I.; Frontiñán-Rubio, J.; Durán-Prado, M.; Peinado, J.R.; Johansson, B.; Alcaín, F.J.; Giménez-Llort, L. Neophobia, NQO1 and SIRT1 as premorbid and prodromal indicators of AD in 3xTg-AD mice. *Behav. Brain Res.* **2014**, *271*, 140–146. [CrossRef]
38. Shen, L.; Chen, Y.; Yang, A.; Chen, C.; Liao, L.; Li, S.; Ying, M.; Tian, J.; Liu, Q.; Ni, J. Redox Proteomic Profiling of Specifically Carbonylated Proteins in the Serum of Triple Transgenic Alzheimer's Disease Mice. *Int. J. Mol. Sci.* **2016**, *17*, 469. [CrossRef] [PubMed]
39. De la Fuente, M. Oxidation and inflammation in the immune and nervous systems, a link between aging and anxiety. In *Handbook of Immunosenescence*; Springer: Berlin/Heidelberg, Germany, 2019; pp. 1–31.
40. Xie, J.; Van Hoecke, L.; Vandenbroucke, R.E. The Impact of Systemic Inflammation on Alzheimer's Disease Pathology. *Front. Immunol.* **2022**, *12*, 796867. [CrossRef]
41. Montacute, R.; Foley, K.; Forman, R.; Else, K.J.; Cruickshank, S.M.; Allan, S.M. Enhanced susceptibility of triple transgenic Alzheimer's disease (3xTg-AD) mice to acute infection. *J. Neuroinflammation* **2017**, *14*, 50. [CrossRef]
42. Munstant, A.; Giménez-Llort, L. Crosstalk of Alzheimer's disease-phenotype, HPA axis, splenic oxidative stress and frailty in late-stages of dementia, with special concerns on the effects of social isolation: A translational neuroscience approach. *Front. Aging Neurosci.* **2022**, *14*, 969381. [CrossRef]
43. Garrido, A.; Cruces, J.; Ceprián, N.; Corpas, I.; Tresguerres, J.A.; De la Fuente, M. Social environment improves immune function and redox state in several organs from prematurely aging female mice and increases their lifespan. *Biogerontology* **2019**, *20*, 49–69. [CrossRef]
44. Barnes, L.L.; Wilson, R.S.; Bienias, J.L.; Schneider, J.A.; Evans, D.A.; Bennett, D.A. Sex differences in the clinical manifestations of Alzheimer disease pathology. *Arch. Gen. Psychiatry* **2005**, *62*, 685–691. [CrossRef]
45. Ferretti, M.; Iulita, M.F.; Cavedo, E.; Chiesa, P.A.; Schumacher Dimech, A.; Santuccione Chadha, A.; Baracchi, F.; Girouard, H.; Misoch, S.; Giacobini, E.; et al. Women's Brain Project and the Alzheimer Precision Medicine Initiative. Sex differences in Alzheimer disease—The gateway to precision medicine. *Nat. Rev. Neurol.* **2018**, *14*, 457–469. [CrossRef] [PubMed]

46. Suarez, L.M.; Diaz-Del Cerro, E.; Felix, J.; Gonzalez-Sanchez, M.; Ceprian, N.; Guerra-Perez, N.; Novelle, M.G.; Martinez de Toda, I.; De la Fuente, M. Sex differences in neuroimmunoendocrine communication. Involvement on longevity. *Mech. Ageing Dev.* **2023**, *211*, 111798. [CrossRef] [PubMed]
47. Yang, J.T.; Wang, Z.J.; Cai, H.Y.; Yuan, L.; Hu, M.M.; Wu, M.N.; Qi, J.S. Sex Differences in Neuropathology and Cognitive Behavior in APP/PS1/tau Triple-Transgenic Mouse Model of Alzheimer's Disease. *Neurosci. Bull.* **2018**, *34*, 736–746. [CrossRef]
48. Kapadia, M.; Mian, M.F.; Michalski, B.; Azam, A.B.; Ma, D.; Salwierz, P.; Christopher, A.; Rosa, E.; Zovkic, I.B.; Forsythe, P. Sex-dependent differences in spontaneous autoimmunity in adult 3xTg-AD mice. *J. Alzheimer's Dis.* **2018**, *63*, 1191–1205. [CrossRef] [PubMed]
49. Kane, A.E.; Shin, S.; Wong, A.A.; Fertan, E.; Faustova, N.S.; Howlett, S.E.; Brown, R.E. Sex differences in healthspan predict lifespan in the 3xTg-AD mouse model of Alzheimer's disease. *Front. Aging Neurosci.* **2018**, *10*, 172. [CrossRef]
50. Dennison, J.L.; Ricciardi, N.R.; Lohse, I.; Volmar, C.H.; Wahlestedt, C. Sexual Dimorphism in the 3xTg-AD Mouse Model and Its Impact on Pre-Clinical Research. *J. Alzheimers Dis.* **2021**, *80*, 41–52. [CrossRef]
51. Baeta-Corral, R.; De la Fuente, M.; Giménez-Llort, L. Sex-dependent worsening of NMDA-induced responses, anxiety, hypercortisolemia, and organometry of early peripheral immunoendocrine impairment in adult 3xTg-AD mice and their long-lasting ontogenic modulation by neonatal handling. *Behav. Brain Res.* **2023**, *438*, 114189. [CrossRef]
52. Barber, A.J.; Del Genio, C.L.; Swain, A.B.; Pizzi, E.M.; Watson, S.C.; Tapiavala, V.N.; Zanazzi, G.J.; Gaur, A.B. Age, sex and Alzheimer's disease: A longitudinal study of 3xTg-AD mice reveals sex-specific disease trajectories and inflammatory responses mirrored in postmortem brains from Alzheimer's patients. *Alzh Res. Ther.* **2024**, *16*, 134. [CrossRef]
53. Meziane, H.; Ouagazzal, A.M.; Aubert, L.; Wietrzych, M.; Krezel, W. Estrous cycle effects on behavior of C57BL/6J and BALB/cByJ female mice: Implications for phenotyping strategies. *Genes. Brain Behav.* **2007**, *6*, 192–200. [CrossRef] [PubMed]
54. Lawrence, R.A.; Burk, R.F. Glutathione peroxidase activity in selenium-deficient rat liver. *Biochem. Biophys. Res. Commun.* **1976**, *71*, 952–958. [CrossRef]
55. Massey, V.; Williams, C.H., Jr. On the reaction mechanism of yeast glutathione reductase. *J. Biol. Chem.* **1965**, *240*, 4470–4480. [CrossRef]
56. Xu, J.; Wang, B.; Ao, H. Corticosterone effects induced by stress and immunity and inflammation: Mechanisms of communication. *Front. Endocrinol.* **2025**, *16*, 1448750. [CrossRef]
57. Cerejeira, J.; Lagarto, L.; Mukaetova-Ladinska, E.B. Behavioral and psychological symptoms of dementia. *Front Neurol.* **2012**, *3*, 73. [CrossRef]
58. Benaroya-Milshtein, N.; Hollander, N.; Apter, A.; Kukulansky, T.; Raz, N.; Wilf, A.; Yaniv, I.; Pick, C.G. Environmental enrichment in mice decreases anxiety, attenuates stress responses and enhances natural killer cell activity. *Eur. J. Neurosci.* **2004**, *20*, 1341–1347. [CrossRef]
59. Deacon, R.M.J.; Rawlins, J.N.P. T-Maze Alternation in the Rodent. *Nat. Protoc.* **2006**, *1*, 7–12. [CrossRef]
60. Giménez-Llort, L.; Ferré, S.; Martínez, E. Effects of the systemic administration of kainic acid and NMDA on exploratory activity 861 in rats. *Pharmacol. Biochem. Behav.* **1995**, *51*, 205–210. [CrossRef] [PubMed]
61. Clinton, L.K.; Billings, L.M.; Green, K.N.; Caccamo, A.; Ngo, J.; Oddo, S.; McGaugh, J.L.; LaFerla, F.M. Age-dependent sexual dimorphism in cognition and stress response in the 3xTg-AD mice. *Neurobiol. Dis.* **2007**, *28*, 76–82. [CrossRef] [PubMed]
62. Dantzer, R. Neuroimmune interactions: From the brain to the immune system and vice versa. *Physiol. Rev.* **2017**, *98*, 477–504. [CrossRef]
63. Leunig, A.; Gianeselli, M.; Russo, S.J.; Swirski, F.K. Connection and communication between the nervous and immune systems. *Nat. Rev. Immunol.* **2025**, *25*, 912–933. [CrossRef] [PubMed]
64. Kim, H.H.; Dixit, V.D. Metabolic regulation of immunological aging. *Nat. Aging* **2025**, *5*, 1425–1440. [CrossRef] [PubMed]
65. Fukushima, Y.; Ueno, R.; Minato, N.; Hattori, M. Senescence-associates T cells in immunosenescence and disease. *Int. Immunol.* **2025**, *37*, 143–152. [CrossRef]
66. Abbas, A.K.; TRotta, E.; Simeonov, D.R.; Marson, A.; Bluestone, J.A. Revisiting IL-1: Biology and therapeutic prospects. *Sci. Immunol.* **2018**, *3*, eaat1482. [CrossRef]
67. Martinez de Toda, I.; Ceprian, N.; Diaz del Cerro, E.; De la Fuente, M. The role of immune cells in oxi-inflamm-aging. *Cells* **2021**, *10*, 2974. [CrossRef]
68. Poulios, P.; Skampouras, S.; Piperi, C. Deciphering the role of cytokines in aging: Biomarker potential and effective targeting. *Mech. Ageing Dev.* **2025**, *224*, 112036. [CrossRef] [PubMed]
69. Al-Shehri, S.S.; Duley, J.A.; Bansal, N. Xanthine oxidase-lactoperoxidase system and innate immunity: Biochemical actions and physiological roles. *Redox Biol.* **2020**, *34*, 101524. [CrossRef]
70. Fraile-Ramos, J.; Dogoh, F.; Ogiator, M.; Oghagbon, E.K.; Giménez-Llort, L. Cognitive impairment and blood biomarkers of renal dysfunction in high-risk Nigerian population, with special attention to women and diabetes. *BMC Neurol.* **2025**, *25*, 158. [CrossRef]

71. Sonsalla, M.M.; Lamming, D.W. Geroprotective interventions in the 3xTg mouse model of Alzheimer's disease. *GeroScience* **2023**, *45*, 1343–1381. [CrossRef]
72. Lopes, P.A.; Guil-Guerrero, J.L. Beyond Transgenic Mice: Emerging Models and Translational Strategies in Alzheimer's Disease. *Int. J. Mol. Sci.* **2025**, *26*, 5541. [CrossRef]
73. Dubal, D.B.; Broestl, L.; Worden, K. Sex and gonadal hormones in mouse models of Alzheimer's disease: What is relevant to the human condition? *Biol. Sex Differ.* **2012**, *3*, 24. [CrossRef] [PubMed]
74. Fertan, E.; Rodrigues, G.J.; Wheeler, R.V.; Goguen, D.; Wong, A.A.; James, H.; Stadnyk, A.; Brown, R.E.; Weaver, I.C.G. Cognitive Decline, Cerebral-Spleen Tryptophan Metabolism, Oxidative Stress, Cytokine Production, and Regulation of the Txnip Gene in a Triple Transgenic Mouse Model of Alzheimer's Disease. *Am. J. Pathol.* **2019**, *189*, 1435–1450. [CrossRef] [PubMed]
75. Ochi, S.; Iga, J.I.; Funahashi, Y.; Yoshino, Y.; Yamazaki, K.; Kumon, H.; Mori, H.; Ozaki, Y.; Mori, T.; Ueno, S.I. Identifying Blood Transcriptome Biomarkers of Alzheimer's Disease Using Transgenic Mice. *Mol. Neurobiol.* **2020**, *57*, 4941–4951. [CrossRef] [PubMed]
76. Kapadia, M.; Mian, M.F.; Ma, D.; Hutton, C.P.; Azam, A.; Narkaj, K.; Cao, C.; Brown, B.; Michalski, B.; Morgan, D.; et al. Differential effects of chronic immunosuppression on behavioral, epigenetic, and Alzheimer's disease-associated markers in 3xTg-AD mice. *Alzheimer's Res. Ther.* **2021**, *13*, 30. [CrossRef]